Gene regulatory patterning codes in early cell fate specification of the *C. elegans* embryo

Alison G. Cole[1*], Tamar Hashimshony[2*], Zhuo Du[3], and Itai Yanai[4]

[1] Department of Molecular Evolution and Development, University of Vienna, Vienna, Austria
[2] Department of Biology, Technion – Israel Institute of Technology, Haifa, Israel.
[3] State Key Laboratory of Molecular Developmental Biology, Institute of Genetics and Developmental Biology, Chinese Academy of Sciences, Beijing, China.
[4] Institute for Computational Medicine, NYU School of Medicine, New York, USA
* These authors contributed equally to this work.

Abstract

Pattern formation originates during embryogenesis by a series of symmetry-breaking steps throughout an expanding cell lineage. In *Drosophila*, classic work has shown that the embryo segmentation is established by morphogens within a syncytium, and the subsequent action of the gap, pair-rule, and segment polarity genes. This classic model however does not translate directly to species that lack a syncytium – such as *C. elegans* – where cell fate is specified by cell-autonomous cell lineage programs and their inter-signaling. Previous single-cell RNA-Seq studies in *C. elegans* have analyzed cells from a mixed suspension of cells from many embryos to study late differentiation stages, or individual early stage embryos to study early gene expression in the embryo. To study the intermediate stages of early and late gastrulation (28- to 102- cells stages) missed by these approaches, here we determine the transcriptomes of the 1- to 102-cell stage to identify 119 embryonic cell-states during cell-fate specification, including 'equivalence-group' cell identities. We find that gene expression programs are modular according to the sub-cell lineages, each establishing a set of stripes by combinations of transcription factor gene expression across the anAterior-posterior axis. In particular, expression of the homeodomain genes establishes a comprehensive lineage-specific positioning system throughout the embryo beginning at the 28-cell stage. Moreover, we find that genes that segment the entire embryo in *Drosophila* have orthologs in *C. elegans* that exhibit sub-lineage specific expression. These results suggest that the *C. elegans* embryo is patterned by a juxtaposition of distinct lineage-specific gene regulatory programs each with a unique encoding of cell location and fate. This use of homologous gene regulatory patterning codes suggests a deep homology of cell fate specification programs across diverse modes of development.

Introduction

Developmental toolkit genes constitute the genomic repertoire that underlies the pathways patterning the organism (Carroll, 2008). These genes are generally involved in signaling transduction modules and transcription factors (TFs) (Degnan et al., 2009; Gerhart, 1999). Their assembly into specific temporal and spatial gene regulatory pathways leads to the specification of cell fates in the embryo. For example, the *C. elegans* endoderm is specified by a cascade of TFs operating sequentially (Maduro and Rothman, 2002). Identifying the principles of gene regulation has been a central endeavor in developmental biology.

John Sulston and colleagues elucidated the 1,340 cells generated throughout the embryogenesis of the nematode *C. elegans*, leading to a hatched worm with 558 cells, each with a described name, lineage, and fate (Sulston et al., 1983). The cell lineage is delineated into a germ-line lineage – P – and five 'founder' somatic cell lineages – AB, MS, E, C, and D – as their each have characteristic cell-cycle timings (Deppe et al., 1978) and cell fates (Fig. 1a). All founder cell lineages are present by the 28-cell stage, when gastrulation initiates, and by the 102-cell stage the progeny of most of the cells have a single fate.

The invariant cell lineage of the *C. elegans* embryo provides an opportunity to systematically study developmental gene pathways. Overall, there are 934 annotated TFs in *C. elegans*, with 40% having experimentally studied DNA-binding specificities (Narasimhan et al., 2015). The overall set can be classified into families according to their DNA-binding domain, including the homeodomain, bHLH, bZIP, T-box, C2H2 zinc finger, and the very large nuclear hormone receptor domain. While mapping the location of signaling pathways is difficult from gene expression data, its effects on the transcriptional output are detectable and consequently studying TF expression provides an entry point into gene expression pathway characterization.

Here, we use single-cell RNA-Seq to identify the transcriptomes of each of the cells up to the 102-cell stage. We find that homeodomain genes are expressed in stripes along the anterior-posterior axis, as early as the 28-cell stage. Interestingly, each founder-cell lineage – AB, MS, C and E – establishes its own regionalization code. These *Drosophila*–like stripe patterns suggest a deep homology in cell fate specification between the embryogenesis of non-segmented and segmented animals, despite differences in syncytium-based and cell-cleavage-based modes of development.

Results

Previous studies analyzed cells from a mixed suspension of cells from different *C. elegans* embryos (Packer et al., 2019). However, this approach does not ensure sampling of each of the individual cells of the early stages, where it is difficult to dissociate the cells. A complementary approach is to manually collect cells by mouth pipette thus ensuring that all cells are collected. Other works employed this approach to study the early stages however only arrived at the 15-cell stage (Hashimshony et al., 2016; Tintori et al., 2016). Up to this stage, few new expressions occur and the transcriptome is dominated by the maternal deposit. As we were interested in studying early specification events in the embryo, we thus manually isolated individual cells from dissociated embryos and processed them for scRNA-Seq (Fig. 1b and Figure S1a). Overall, we studied 840 cells from 38 embryos up to the 102-cell stage, collecting all or most cells of each embryo (Fig. 1b and Table S1).

Analyzing the transcriptomes, we found that embryo-to-embryo variation could be efficiently normalized by standardizing each gene's expression across all cells collected from the same embryo (*i.e.*, mean of zero and standard deviation of one; see Methods). This is another benefit of the manual collection approach. A dimensional reduction map of the examined cells (Fig. 1b) reveals the unfolding of development with cells from the early stages occupying the center while cells from later stages occupy the periphery. We found that cells followed developmental trajectories according to their founder cell origin, each identified by the expression of genes known to be expressed in a lineage-specific manner: *ceh-51* (MS), *elt-7* (E), *pal-1* (C,D and P), *pes-1* (D) and *nos-2* (P) (Fig. 1c) (Broitman-Maduro et al., 2009; Hunter and Kenyon, 1996; Lee et al., 2017; Maduro and Rothman, 2002). As also observed by other studies (Packer et al., 2019), the founder cell lineage trajectories are oriented according to cell fates, with similar cell fates converging between lineages (Fig. 1b,d): the cells of the ecto-mesoderm producing C lineage formed a bi-lobed cloud with the muscle part adjacent to that of the MS and D lineages. Similarly, MS cells that will form the pharynx orient towards the pharynx producing portion of the AB lineage.

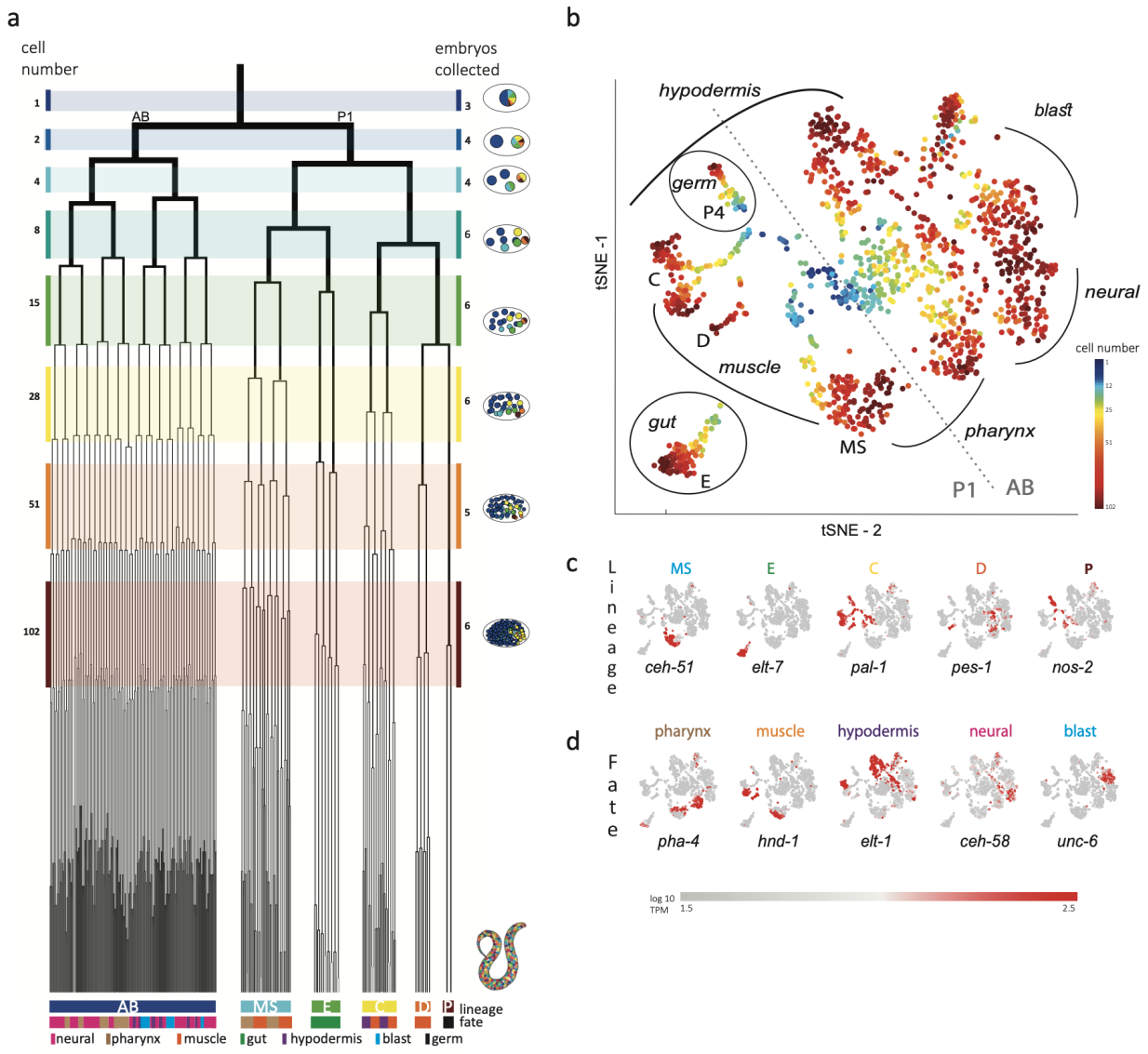

Figure 1: Single-cell transcriptomics in the early *C. elegans* embryo. a, The embryonic *C. elegans* cell lineage as deciphered by Sulston and colleagues (Sulston et al., 1983). The number of cells present at each stage is indicated on the left and schematic images of the embryo are shown for several stages to the right with cells colored by founder cell lineages AB, MS, E, C, D, and P. The fate of the cells at the last stage is also indicated according to the legend at the foot of the lineage. The number of embryos examined in this study is indicated on the right. Colored bars correspond to the windows in which embryos were considered to be at the same stage. **b,** a tSNE map of the cells isolated in this study. Circles indicate the individual cells, colored by the stage of development of the embryo from which they were manually collected. **c-d,** Gene expression for the indicated lineage and fate marker genes on the tSNE map shown in **b**.

In order to infer the precise identity of each cell, we first organized the embryos into eight developmental stages: the 1-, 2-, 4-, 8-, 15-, 28-, 51-, and 102-cell stages (Fig. 1a). For each stage, we studied cells from multiple embryos and identified clusters of cells according to differential gene expression. Figure 2a demonstrates this analysis for the 15-cell stage and Figure S1b for all other stages. The identified clusters contain cells from each of the individual embryos, thus confirming our underlying assumption that embryo to embryo gene expression variation is minimal relative to the coherence of the cell states within an embryo. Finally, we inferred the cell identity of each cluster with reference to known gene markers from the literature (Tables S2,3). Figure 2b illustrates our approach for the cells of the 28-cell stage (see Fig. S2 for all other stages). New markers were required to distinguish some of the cell identities. Studying *F19F10.1* by single molecule FISH, we found that this previously uncharacterized ets-factor is expressed in the posterior daughter cell through 2 cell cycle divisions (Fig. 2c). We further tested for the robustness of the cell identity assignments and ensured that each cell is most similar to its assigned identity (computed with itself excluded, Fig. S2, bottom of each subfigure). We identified 5,433 genes as being differentially expressed within a stage, collectively across all of the stages (see Methods). Of these, 395 are TFs during this period of cell specification (Table S6).

For some cell identities within a stage we were not able to distinguish distinct transcriptomes, and we thus denoted these as composing 'equivalence groups'. These may either be attributed to daughter cells whose transcriptomes have yet to diverge, such as cells Ca and Cp in the 15-cell state, or to sets of cousins whose sub-lineages form repeating units, such as cells ABplp and ABprp (also of the 15-cell stage) (Sulston et al., 1983). In the first case, this indicates that sister-cells are transcriptomically very similar shortly after division. Altogether we describe 119 cell identities with distinct transcriptome profiles, which by stage are as follows: 1 (1-cell), 2 (2-cell), 4 (4-cell), 6 (8-cell), 11 (15-cell), 20 (28-cell), 38 (51-cell), and 37 (102-cell), with 64 of these representing equivalence groups of at least two cell states (Fig. 2d, Table S5, and Fig. S3). For each cell state that we assigned, we have an average of seven replicate cells (Table S4). We validated our annotations by imaging GFP reporters and found good correspondence, as illustrated for *ceh-43*, *dmd-4* and *unc-30* (Fig. 2e and Fig. S4). The delay between the GFP-expression and the mRNA detected here is expected as previously described (Murray et al., 2012).

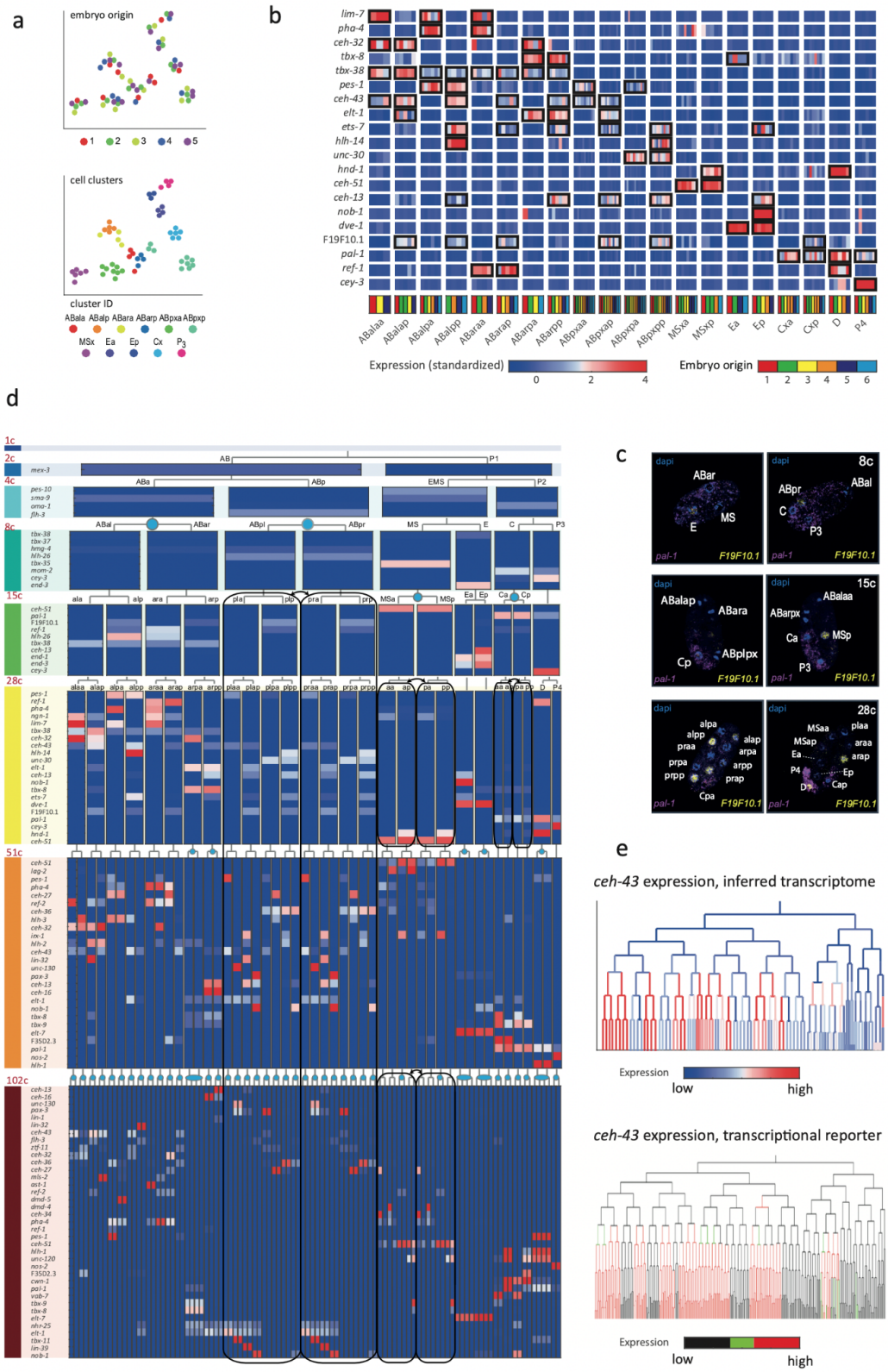

Figure 2: Inferring the transcriptomes of cell states throughout specification in the *C. elegans* embryo. a, tSNE clusters of cells from 15-cell stage embryos, shown in terms of their

embryo of origin (top), cell clustering (middle) and inferred cell identity (bottom). **b,** Gene expression for the indicated genes across the assigned cell states of the 28-cell stage. Rows correspond to genes and each bar within a cell state indicates the expression level of a sample. Black boxes indicate differential gene expression. Colors in the bottom row indicate the embryo of origin. **c,** Double single-molecule RNA *in situ* hybridization showing spatial identity of *F19F10.1* expressing nuclei (yellow). The positions of all nuclei are shown with DAPI-staining (blue), and the embryos were oriented with the posterior landmark gene *pal-1* (purple) (Hunter and Kenyon, 1996). Cell identities were manually annotated based on previous descriptions (Table S4). **d,** Average expression of cluster identity genes through the first 8 cell-divisions of embryonic development. Each bar represents the inferred transcriptome of a cell state and shows the standardized expression for the indicated genes, using the same color bar as in **b**. Equivalent transcriptomes derived from sister cells are indicated by blue circles. Lineage symmetry gives rise to left/right equivalence groups indicated with black boxes. **e,** Expression of *ceh-43* according to lineage of the inferred transcriptomes (top) and a transcriptional reporter strain (bottom), where highest expression is shown in red and no detected expression is black (see also Fig. S4).

We next asked if the genes that are members of the same gene family have similar spatial and temporal expression arrangements. To test for this mode of expression, we considered groups of genes with the same DNA binding domain, as annotated by the PFAM database (Finn et al., 2016). For each cell, we queried for enrichments or depletions of genes of specific domain families, among its expressed TFs. As an example, the 'ABplppp' cell differentially expresses 14 TFs according to our analysis, including seven homeobox domain (HDs) TFs, though overall HDs only account for 11% of the TFs (Fig. 3a). We used the hypergeometric distribution to compute a significance of $P = 0.00015$ for this overlap, given the overall number of TFs and the number of HD and 'ABplppp' TFs. Conversely, only two of the 69 TFs expressed by the Eala cell are HDs, a significant depletion (P=0.01, Hypergeometric distribution). Figure 3b shows the overall pattern of enrichments and depletions of HDs across all of the examined cells, indicating enrichment of HDs in the 51-cell stage, in particular in the ABp lineage, and depletion in the E lineage. For the GATA type zinc factors we found enrichment in the E lineage, as well as some of the AB cells (Fig. 3c).

Examining the pattern of such biases, we found that TF families showed significant enrichments across lineages and developmental stages (Fig. 3d-e). Four TF gene families are enriched in the AB lineage: the T-box domain, the helix-loop-helix (HLH) DNA-binding domain, the HD domain, and the high mobility group (HMG) box domain (Fig. 3d). Each of these families also has enrichments for specific AB stages, from early expression (T-box and HLH) to later expression (HD and HMG).

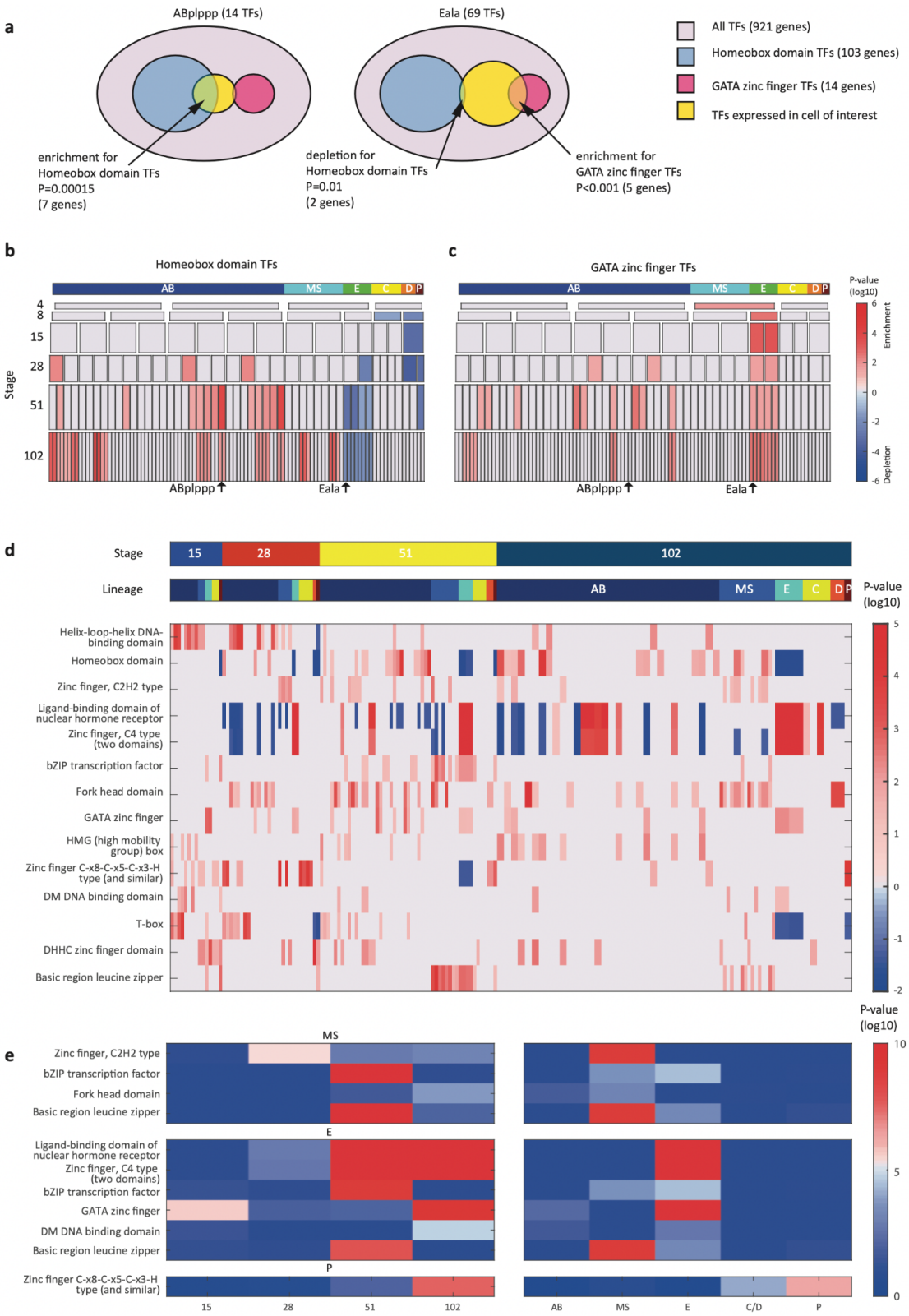

Figure 3: TF gene families have spatiotemporal specificities. a, Detecting enrichment and depletion of genes of the same gene family, among the TFs expressed by a cell, using the

hypergeometric distribution. **b-c,** For the homeobox domain (**b**) and GATA zinc finger domain (**c**) gene families, the enrichments and depletions are indicated for each cell of the lineage, plotted as in Fig. 2d. **d,** TF family stage and lineage enrichments. For each cell (column), the enrichment and depletion for the genes of a TF family (row) is indicated (similar to **b,c**). The top bars indicate the lineage and stage of the cell. **e,** For the indicated TF family the significance for enrichments is shown using the T-test between the values shown in **d** for the noted stage and lineage.

From the Figure 3 analysis we concluded that the homeodomain (HD) TF family in particular exhibited lineage-specific expression. Studying this in more detail, we observed that in the 28-cell stage, each of the 16 AB cells contains expression of at least one homeodomain gene, with 8 distinct cell state patterns (Fig. 4a). This is mostly also apparent in the 51- and 102-cell stages. The expression patterns of all homeodomain genes across the lineage are not mono-phyletic. For example, *ceh-43* is expressed in nine of the sixteen AB cells at the 28-cell stage in a complex pattern (Fig. 4a). Thus, continuous symmetry breaking (Zacharias and Murray, 2016), does not appear to be a mechanism by which differential expression is generally established.

We asked if the relative spatial location of the cells within the embryo can provide insight into the observed homeodomain expression patterns. For this analysis, we mapped the binarized expression of genes onto the known three dimensional locations of cells in the embryo. Studying the 28-cell stage, we found that the homeodomain genes expressed in each lineage revealed dorsal-ventral stripes along the anterior-posterior axis (Fig. 4b). For example, the *ceh-43*-expressing cells, deriving from distinct AB sub-lineages, are physically proximate. Clustering the AB lineage cells into eight groups according to their binarized expression, we mapped the gene expression combinations of each stripe. One stripe, for example, includes the expression of *unc-30*, *ceh-36*, and *ceh-13*; the adjacent stripe has expression of *unc-30*, *ceh-36*, and *mec-3* (Fig. 4b). At the 51-cell stage, 4 new homeodomain genes are expressed in the AB lineage, and again position along the anterior-posterior axis correlates with gene expression. In the 102-cell stage, expression becomes more complicated as the AB lineage forms an external shell around the gastrulating non-AB cells. Generalizing this approach, we also found distinct positional systems for the MS and C lineages (Fig. 4b,c). For the MS lineage, *ceh-32* and ceh-51 are in the anterior and posterior, respectively, while for the C lineage *vab-7* (even-skipped) and *hmbx-1* are in the anterior and posterior, respectively. We thus provide evidence that distinct regionalization codes occur across the embryonic sub-lineages.

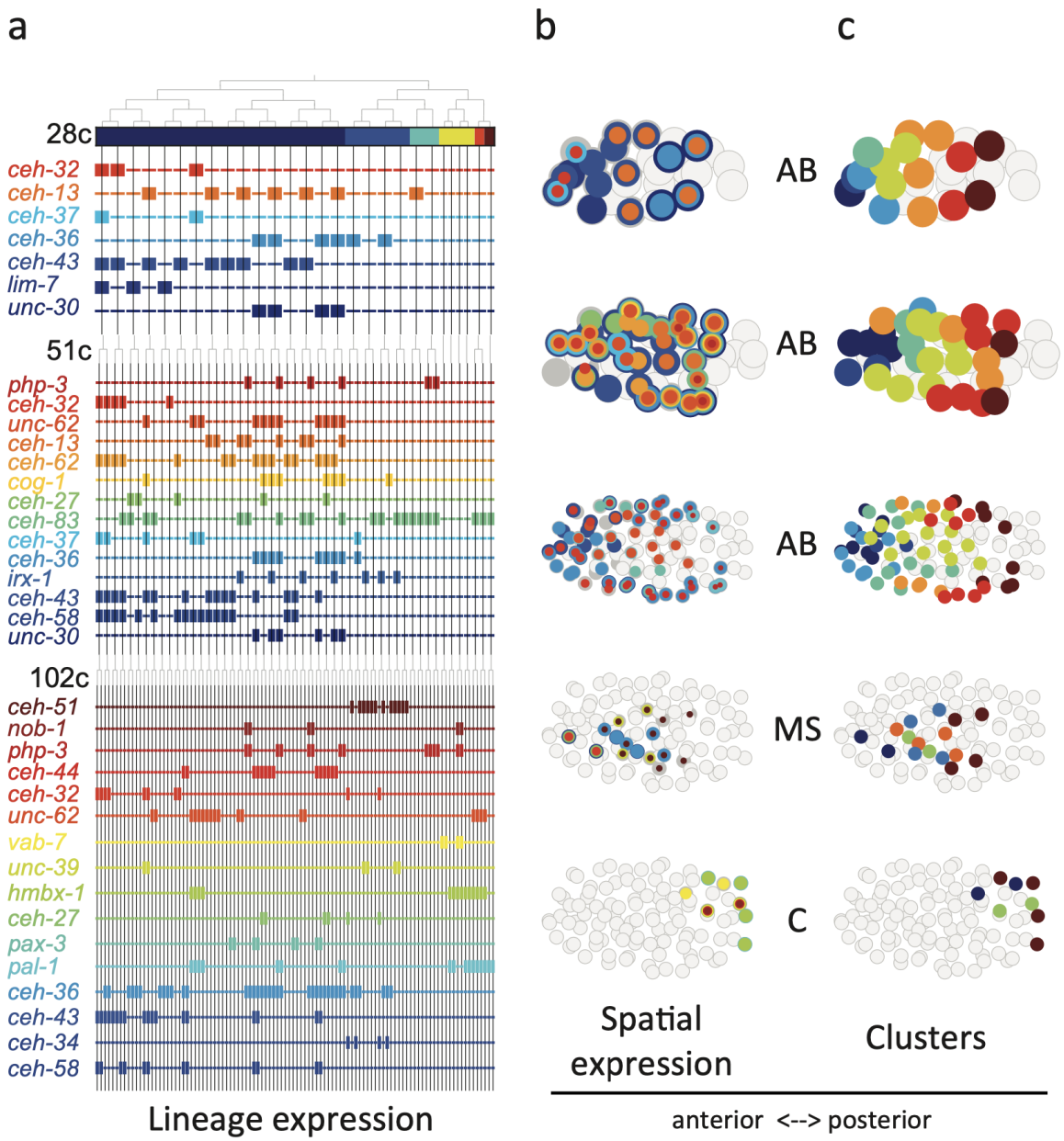

Figure 4: Homeodomain genes are expressed in lineage-specific stripes across the anterior-posterior axis. a, Lineage expression patterns for the indicated genes in the 28-, 51-, and 102-cell stage. Thick and thin lines indicate binarized 'on' and 'off' expression, respectively. **b,** Three dimensional expression patterns separated by lineage (AB/MS/C) for the genes indicated in **a**. Circles represent cells in the embryo at the particular stage examined. Expression of each gene is indicated by a circle of a different size and color. Light gray cells indicate cells in other lineages. **c,** Clustering of cells according to gene expression of the indicated lineage and stage. Colors distinguish K-means clustering.

To compare the patterning code elucidated for *C. elegans* embryogenesis to the well-studied patterning pathway in *Drosophila*, we also studied the expression of *C. elegans* orthologous genes. *Drosophila* development proceeds through a series of molecular events which partition the syncytial embryo along the anterior-posterior axis (Wolpert et al., 2019). We found that the *C. elegans* genes such as *nos-1,2* (*nanog*) and *puf* genes (*pumilo*) which are maternal genes in both systems – are restricted to the primary germ cell lineage in *C. elegans* (Fig. 5). Moreover, gap and pair-rule genes, such as *pal-1* (*caudal*) and *cwn-1* (*wg*), show C lineage and sub-lineage restriction, respectively (Fig. 5). Thus, it is evident that while *Drosophila* patterning follows in a lineage-independent manner, in *C. elegans*, lineage-dependency is co-incident with specific expression of patterning genes across the founder-cell lineages (Fig. S5).

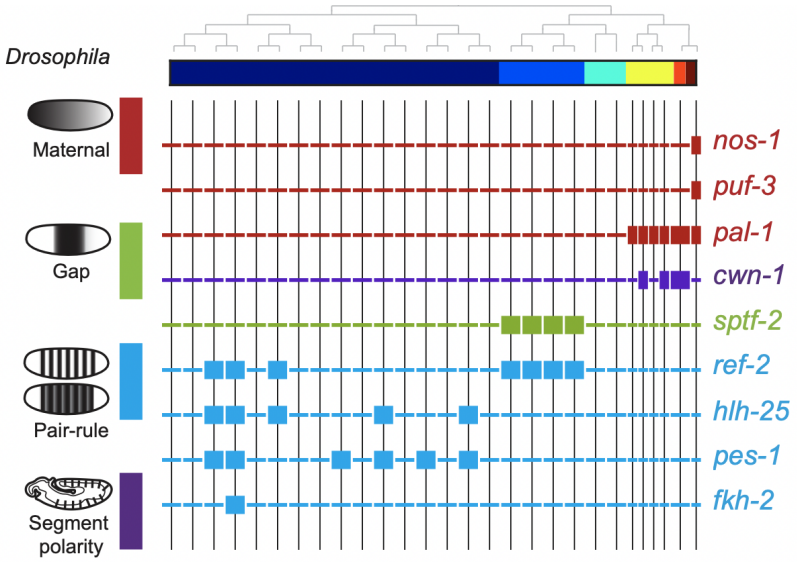

Figure 5. Expression of the orthologs of *Drosophila* specification genes in *C. elegans*. Lineage expression patterns in the 28-cell stage for the indicated genes whose orthologs function as maternal, gap, pair-rule, and segment polarity genes in *Drosophila*. Thick and thin lines indicate binarized 'on' and 'off' differential expression, respectively.

Discussion

Collectively, our analysis reveals that during embryogenesis, in between the early signaling period – involving *Notch* (Priess, 2005) and *Wnt* (Rocheleau et al., 1997; Thorpe et al., 1997)– and the later cell-fate differentiation period – involving myogenic factors such as *myoD/hlh-1* (Chen et al., 1992) and *GATA/elt-2* (Fukushige et al., 1998) – there is a period of lineage-specific patterning. Three of the homeodomain genes whose expression we have described – *ceh-13*, *php-3*, and *nob-1* (Fig. 4) – are members of the HOX sub-family, known to provide regionalization during embryogenesis in bilaterians (Carroll et al., 2004). Indeed, we observed that expression of these HOX genes transcends the founder lineages and patterns the posterior region in multiple lineages (Fig. 4). However, we find 51 other homeodomain genes that pattern the lineages and set up locations in the embryo. This is an increased genetic repertoire relative to *Drosophila* (97 to 104, respectively) despite the higher complexity of the latter in terms of cell-types and total number of cells. Thus, in species where regionalization is under lineage control, as opposed to morphogen gradients, there is a greater necessity for distinct positional systems across distinct sub-lineages – here the founder-cell lineages. We find lineage-specific gene expression stripes (Fig. 4), suggesting that such a developmental patterning mechanism may not be restricted to segmented organisms but is rather a fundamental feature of animal embryogenesis. The centrality of homeodomain genes to this system highlights the adaptability of this TF family to both lineage-dependent and position-dependent functions. It will be interesting to further compare other species at the single-cell level in order to trace the evolutionary origin of gene expression developmental patterning codes.

Methods

Cell isolations. Embryos were isolated from adult worms and removed from their egg shells as described in Edgar and Goldstein (Edgar and Goldstein, 2012). Individual embryos were manually dissociated by gentle pipetting through progressively smaller glass-bore pipettes in Calcium/Magnesium free EGM. Cell losses during dissociation were noted and single dissociated cells from an individual embryo were counted, collected as previously described (Hashimshony et al., 2012), and stored at -80C until further processing.

Single-cell RNA-Seq. Individual embryo, multiplexed single-cell RNA sequencing libraries were produced following the CEL-Seq2 protocol (Hashimshony et al., 2016). Briefly, individually

harvested cells were barcoded with a reverse transcription reaction, and RNA molecules were tagged with unique molecular identifiers (UMIs) (Kivioja et al., 2011). All barcoded cells from a single embryo were then combined into a single IVT amplification reaction which was used to generate an Illumina library for sequencing. Multiple sequencing libraries with compatible Illumina sequencing indexes were sequenced together on an Illumina HiSeq 2500 using standard paired-end sequencing protocols. For Read 1, used to determine the barcode, the first 15 bp were sequenced and for Read 2, used to determine the identity of the transcript, the first 35 bp were sequenced. The CEL-Seq2 pipeline is available at https://github.com/yanailab/CEL-Seq-pipeline. Mapping of the reads used BWA33, version 0.6.1, against the C. elegans WBCel215 genome (bwa aln -n 0.04 -o 1 -e -1 -d 16 -i 5 -k 2 -M 3 -O 11 -E 4). Read counting used htseq-count version 0.5.3p1 defaults, against WS230 annotation exons.

Initial processing of the CEL-Seq2 data. Gene expression values were calculated as UMI-corrected reads normalized to the number of transcripts per 50,000; only cells with more than 10,000 mapped reads were included in the analysis. In order to compare gene expression patterns between embryos, gene expression was first standardized among the cells of an individual embryo (such that the mean expression for each gene across the cells of the embryo is 0 and the standard deviation is 1), and these standardized expression profiles were used for comparisons between embryos.

Cell clustering. t-Distributed Stochastic Neighbor Embedding (tSNE)(van der Maaten and Hinton, 2008) was performed on full dataset using the top 1000 most variable genes (according to the fano factor), with 20 initial dimensions and perplexity set at 50. For reproducibility, a non-random initiation of the objective function was set (https://lvdmaaten.github.io/tsne/).

Cell identity inference. For each of the eight examined stages – 1-cell, 2-cell, 4-cell, 8-cell, 15-cell, 28-cell, 51-cell, and 102-cell – the isolated cells were first clustered according to their position on a tSNE plot using genes of known expression patterns (Table S2). We next manually and iteratively accepted clusters based upon their homogenous embryo composition, by removing the accepted cluster and re-clustering the remaining cells. These clusterings were based upon the restricted set of genes with known cell identity (Table S2). Cell state was then annotated to the clusters by comparing the average gene expression of the cluster with a collated database of known gene expression patterns (Table S3). The robustness of the

clustering was tested by only retaining cells whose expression is most similar to the mean expression of each cluster, computed without it (Fig. S2). The cell state transcriptome was then computed as the average expression of all members, together with standard deviation (Table S6).

FISH analysis. Custom Stellaris FISH probe sets were designed against the entire coding sequence of *F19F10.1* (25 non-overlapping probes labeled with CAL Fluor Orange 560 Dye) and pal-1 (25 non-overlapping probes labeled with C3-Fluorescein Dye), using the Stellaris FISH Probe Designer (Biosearch Technologies, Inc., Petaluma, CA: www.biosearchtech.com/stellarisdesigner). Fluorescent in situ hybridization (FISH) was performed according to the protocol available on the Stellaris web-site (https://www.biosearchtech.com/support/resources/stellaris-protocols) for fixation of embryonic *C. elegans* material, with the following modification: all steps were performed in 1.5mL Eppendorf tubes. Hybridization of two non-overlapping probe sets was performed using 125 nM of each probe set contemporaneously. Within 48hrs from completing the hybridization protocol, embryos were mounted on glass slides under #0 coverglass (85-115 uM thickness), supported on each corner by small amounts of plasticine to avoid crushing the embryos. Slides were imaged immediately after mounting with a Zeiss LSM 510 confocal microscope.

Lineage tracing and single-cell fluorescence quantification. Embryo mounting and live imaging were performed as previously described45. Briefly, 2-4 cell stage embryos were mounted between two cover slips in M9 buffer containing 20 μm microspheres (Polyscience). Dual-color 3D time-lapse imaging was performed using a Spinning disc confocal microscopy. Images were acquired with 30 focal planes at 1 μm Z resolution for every 75 seconds during a six-hour duration of embryogenesis. Ubiquitously expressed mCherry was used for automated cell identification and lineage tracing using StarryNite program followed by systematic manual correction of errors(Santella et al., 2014). Protein fusion GFP was used to quantify expression level of corresponding gene in each cell using a previous established method(Murray et al., 2008). GFP intensity was measured by calculating the average GFP intensity for each cell and then with the local background intensity subtracted. GFP intensity at different time point for a same cell was averaged to quantify expression level of a gene in a cell.

Differential gene expression analysis. For each gene, at each stage, we identified differential gene expression using the following approach. We compared the standardized gene expression

values across the cell states of the stage, and identified the two groups of cell states that correspond to the most significantly different groups, assayed by a t-test P-value. In order to establish the significance, we then asked if that P-value is better than that expected by shuffling the expression values across states. To find the two groupings with the best P-value, we began by computing a t-test between the expression values for each cell state and the rest of the expression levels of the remaining states. The cell state with the best P-value was used to seed a group and we next computed the P-value of a super-group composed of this cell state in turn with each other cell state, comparing with the expression values of the remaining cell states. If one of these super-groups had a better P-value than the original best P-value state alone, we selected it and continued this process, iteratively adding to the super-group until the P-value can no longer improve. This process results in a one cell state or a super-group of cell states with expression and a group without expression. Each gene will thus have a binary profile and an associated P-value. To select the genes with sufficiently significant P-values we repeated the procedure on 10,000 shuffled sample to cell state assignments. Sorting the P-values from the shufflings, the P-value at 1% of this list was used as the threshold, for a false discovery rate of 1%. We excluded differential expression of genes expressed in more than 50% of the cells of a given stage, and also restricted differential expression to those genes whose maximum expression is at least three quarters of a $\log_{10}$ TPM unit greater than the minimum expression at the given stage.

Enrichments and depletions of TF families in cells. For each cell, we computed both the enrichment and depletion of the set of genes in a given TF family among its expressed TFs. The enrichment and depletion is computed as the cumulative hypergeometric P-value with and without subtracted from unity, respectively. The smallest number between these two tests distinguishes an enrichment from a depletion (see Fig. 3a), and we multiplied the –log10 P value by 1 and -1, to distinguish these in the plots shown in Figure 3b,c. To compute the significance of enrichments for particular lineages and stages, we used the T-test on the –log10 P-values of the enrichment values.

References

Broitman-Maduro G, Owraghi M, Hung WWK, Kuntz S, Sternberg PW, Maduro MF. 2009. The NK-2 class homeodomain factor CEH-51 and the T-box factor TBX-35 have overlapping function in C. elegans mesoderm development. *Development* **136**:2735–2746.

Carroll SB. 2008. Evo-devo and an expanding evolutionary synthesis: a genetic theory of morphological evolution. *Cell* **134**:25–36.

Carroll SB, Grenier JK, Weatherbee SD. 2004. From DNA to Diversity: Molecular Genetics and the Evolution of Animal Design. Wiley.
Chen L, Krause M, Draper B, Weintraub H, Fire A. 1992. Body-wall muscle formation in Caenorhabditis elegans embryos that lack the MyoD homolog hlh-1. *Science* **256**:240–243.
da Veiga Beltrame E, Arnaboldi V, Sternberg PW. 2022. WormBase single-cell tools. *Bioinform Adv* **2**:vbac018.
Degnan BM, Vervoort M, Larroux C, Richards GS. 2009. Early evolution of metazoan transcription factors. *Curr Opin Genet Dev* **19**:591–599.
Deppe U, Schierenberg E, Cole T, Krieg C, Schmitt D, Yoder B, von Ehrenstein G. 1978. Cell lineages of the embryo of the nematode Caenorhabditis elegans. *Proc Natl Acad Sci U S A* **75**:376–380.
Edgar LG, Goldstein B. 2012. Culture and manipulation of embryonic cells. *Methods Cell Biol* **107**:151–175.
Finn RD, Coggill P, Eberhardt RY, Eddy SR, Mistry J, Mitchell AL, Potter SC, Punta M, Qureshi M, Sangrador-Vegas A, Salazar GA, Tate J, Bateman A. 2016. The Pfam protein families database: towards a more sustainable future. *Nucleic Acids Res* **44**:D279–85.
Fukushige T, Hawkins MG, McGhee JD. 1998. The GATA-factor elt-2 is essential for formation of the Caenorhabditis elegans intestine. *Dev Biol* **198**:286–302.
Gerhart J. 1999. 1998 Warkany lecture: signaling pathways in development. *Teratology* **60**:226–239.
Hashimshony T, Senderovich N, Avital G, Klochendler A, de Leeuw Y, Anavy L, Gennert D, Li S, Livak KJ, Rozenblatt-Rosen O, Dor Y, Regev A, Yanai I. 2016. CEL-Seq2: sensitive highly-multiplexed single-cell RNA-Seq. *Genome Biol* **17**:77.
Hashimshony T, Wagner F, Sher N, Yanai I. 2012. CEL-Seq: single-cell RNA-Seq by multiplexed linear amplification. *Cell Rep* **2**:666–673.
Hunter CP, Kenyon C. 1996. Spatial and temporal controls target pal-1 blastomere-specification activity to a single blastomere lineage in C. elegans embryos. *Cell* **87**:217–226.
Kivioja T, Vähärautio A, Karlsson K, Bonke M, Enge M, Linnarsson S, Taipale J. 2011. Counting absolute numbers of molecules using unique molecular identifiers. *Nat Methods* **9**:72–74.
Lee C-YS, Lu T, Seydoux G. 2017. Nanos promotes epigenetic reprograming of the germline by down-regulation of the THAP transcription factor LIN-15B. *Elife* **6**. doi:10.7554/eLife.30201
Maduro MF, Rothman JH. 2002. Making worm guts: the gene regulatory network of the Caenorhabditis elegans endoderm. *Dev Biol* **246**:68–85.
Murray JI, Bao Z, Boyle TJ, Boeck ME, Mericle BL, Nicholas TJ, Zhao Z, Sandel MJ, Waterston RH. 2008. Automated analysis of embryonic gene expression with cellular resolution in C. elegans. *Nat Methods* **5**:703–709.
Murray JI, Boyle TJ, Preston E, Vafeados D, Mericle B, Weisdepp P, Zhao Z, Bao Z, Boeck M, Waterston RH. 2012. Multidimensional regulation of gene expression in the C. elegans embryo. *Genome Res* **22**:1282–1294.
Narasimhan K, Lambert SA, Yang AWH, Riddell J, Mnaimneh S, Zheng H, Albu M, Najafabadi HS, Reece-Hoyes JS, Fuxman Bass JI, Walhout AJM, Weirauch MT, Hughes TR. 2015. Mapping and analysis of Caenorhabditis elegans transcription factor sequence specificities. *Elife* **4**. doi:10.7554/eLife.06967
Packer JS, Zhu Q, Huynh C, Sivaramakrishnan P, Preston E, Dueck H, Stefanik D, Tan K, Trapnell C, Kim J, Waterston RH, Murray JI. 2019. A lineage-resolved molecular atlas of embryogenesis at single-cell resolution. *Science* **365**. doi:10.1126/science.aax1971
Priess JR. 2005. Notch signaling in the C. elegans embryo. *WormBook* 1–16.
Rocheleau CE, Downs WD, Lin R, Wittmann C, Bei Y, Cha YH, Ali M, Priess JR, Mello CC. 1997. Wnt signaling and an APC-related gene specify endoderm in early C. elegans embryos. *Cell* **90**:707–716.
Santella A, Du Z, Bao Z. 2014. A semi-local neighborhood-based framework for probabilistic cell

lineage tracing. *BMC Bioinformatics* **15**:217.
Sulston JE, Schierenberg E, White JG, Thomson JN. 1983. The embryonic cell lineage of the nematode Caenorhabditis elegans. *Dev Biol* **100**:64–119.
Thorpe CJ, Schlesinger A, Carter JC, Bowerman B. 1997. Wnt signaling polarizes an early C. elegans blastomere to distinguish endoderm from mesoderm. *Cell* **90**:695–705.
Tintori SC, Osborne Nishimura E, Golden P, Lieb JD, Goldstein B. 2016. A Transcriptional Lineage of the Early C. elegans Embryo. *Dev Cell* **38**:430–444.
van der Maaten L, Hinton G. 2008. Visualizing Data using t-SNE. *J Mach Learn Res* **9**:2579–2605.
Wolpert L, Tickle C, Arias AM, Locke J. 2019. Principles of Development. Oxford University Press.
Zacharias AL, Murray JI. 2016. Combinatorial decoding of the invariant C. elegans embryonic lineage in space and time. *Genesis* **54**:182–197.

Acknowledgements: We thank the Technion Genome Center. This work was supported by a European Research Council grant (EvoDevoPaths). We are grateful for the EPIC2 dataset, which we used extensively.

Author Contributions: A.G.C., T.H., and I.Y. conceived and designed the project. A.G.C. led the collection of cells, T. H. led their sequencing with CEL-Seq2. Processing of CEL-Seq2 reads and initial bioinformatics was performed by A.G.C. Z.D. contributed the fusion-protein imaging analysis. The data analysis was led by I.Y. with significant contributions from A.G.C. and with help from T.H. I.Y. drafted the manuscript which the authors commented on.

Author information: The complete data set has been deposited to the NCBI GEO database GSE70185. The authors declare no competing financial interests. Correspondence and requests for materials should be addressed to I.Y. (itai.yanai@nyulangone.org).

SUPPLEMENTARY FIGURES

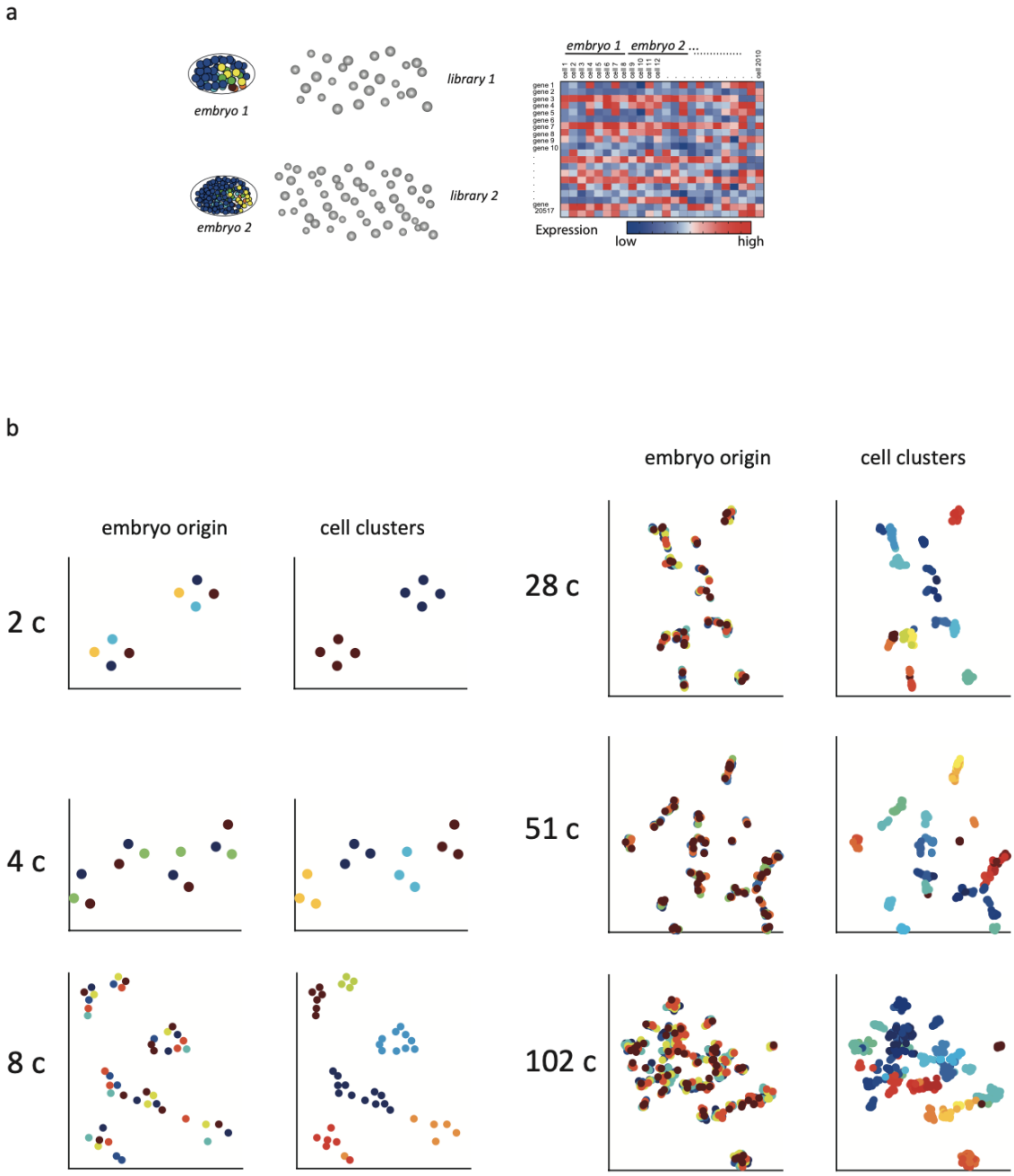

Figure S1: Sample collection and initial analysis. a, A schematic indicating how transcriptomes are collected. Individual embryos are opened and the cells were manually isolated such that for each cell the embryo of origin is also recorded. **b,** tSNE plots for the indicated cell stages. (left) Cells are colored by embryo of origin. (right) Cells are colored by inferred cell-fate.

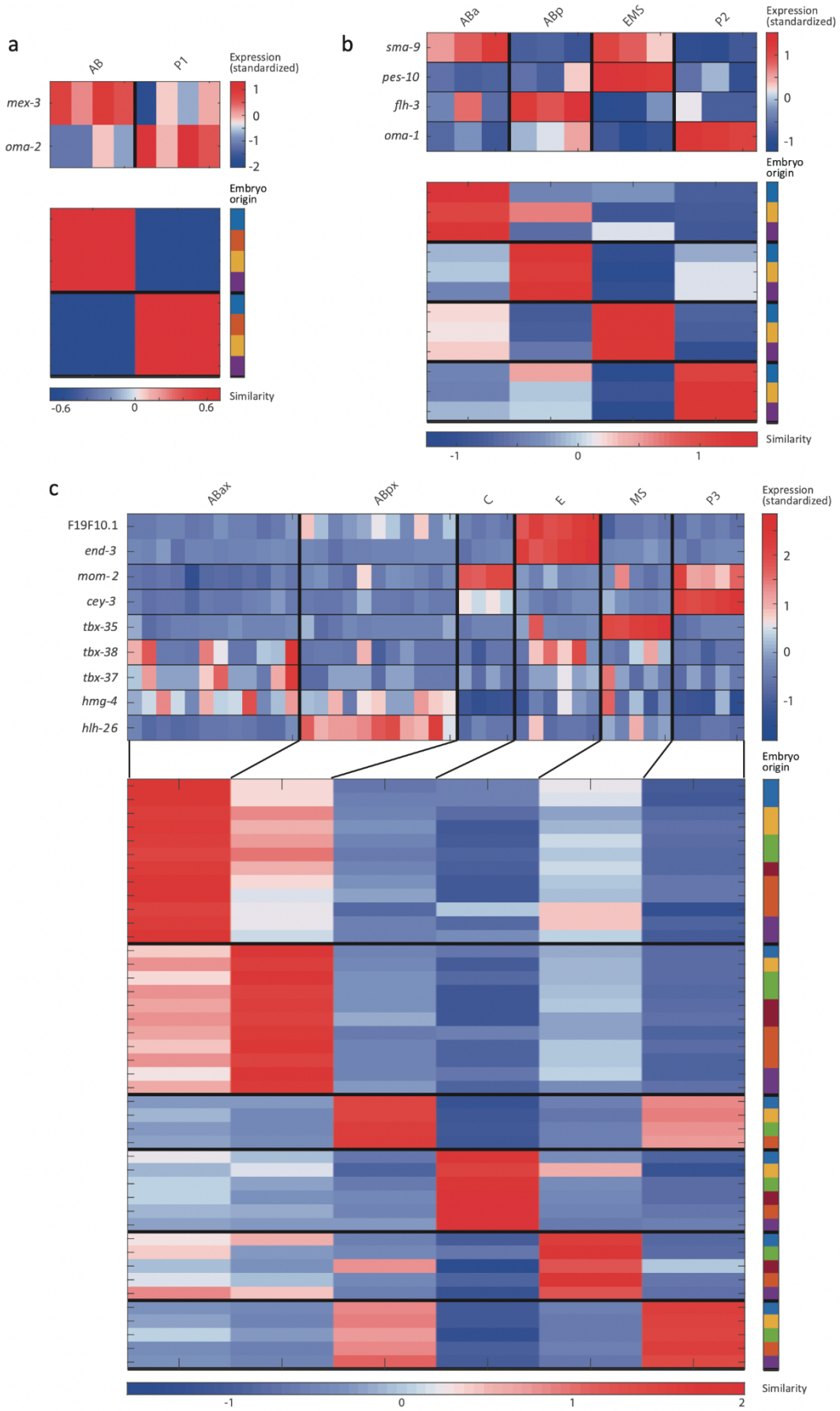
a
AB
P1
Expression (standardized)
mex-3
oma-2
1
0
-1
-2
Embryo origin
Similarity
-0.6
0
0.6
b
ABa
ABp
EMS
P2
Expression (standardized)
sma-9
pes-10
flh-3
oma-1
1
0
-1
Embryo origin
Similarity
-1
0
1
c
ABax
ABpx
C
E
MS
P3
Expression (standardized)
F19F10.1
end-3
mom-2
cey-3
tbx-35
tbx-38
tbx-37
hmg-4
hlh-26
2
1
0
-1
Embryo origin
Similarity
-1
0
1
2

Figure S2

d

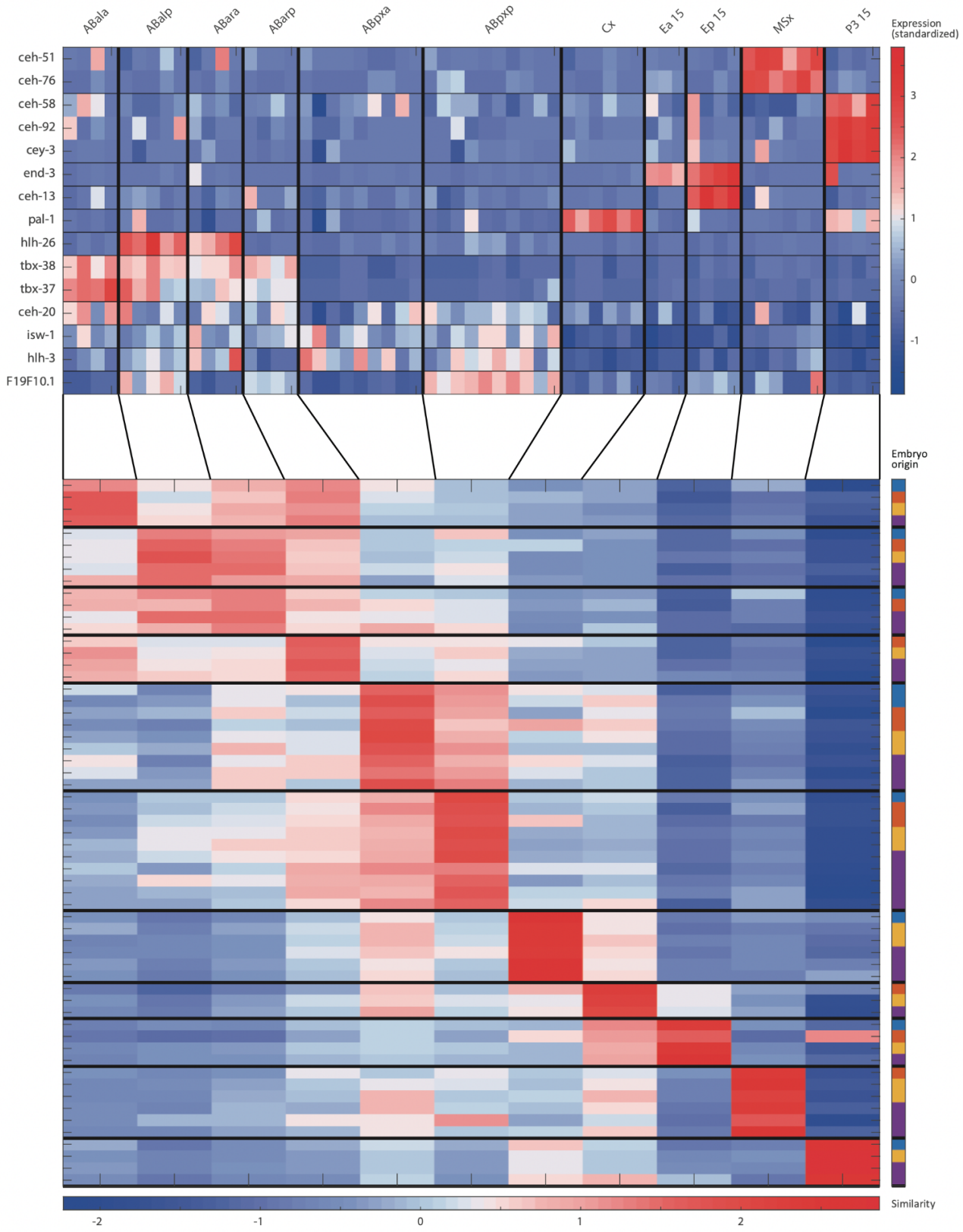
ABala
ABalp
ABara
ABarp
ABpxa
ABpxp
Cx
Ea 15
Ep 15
MSx
P3 15
Expression (standardized)
3
2
1
0
-1
ceh-51
ceh-76
ceh-58
ceh-92
cey-3
end-3
ceh-13
pal-1
hlh-26
tbx-38
tbx-37
ceh-20
isw-1
hlh-3
F19F10.1
Embryo origin
Similarity
-2
-1
0
1
2

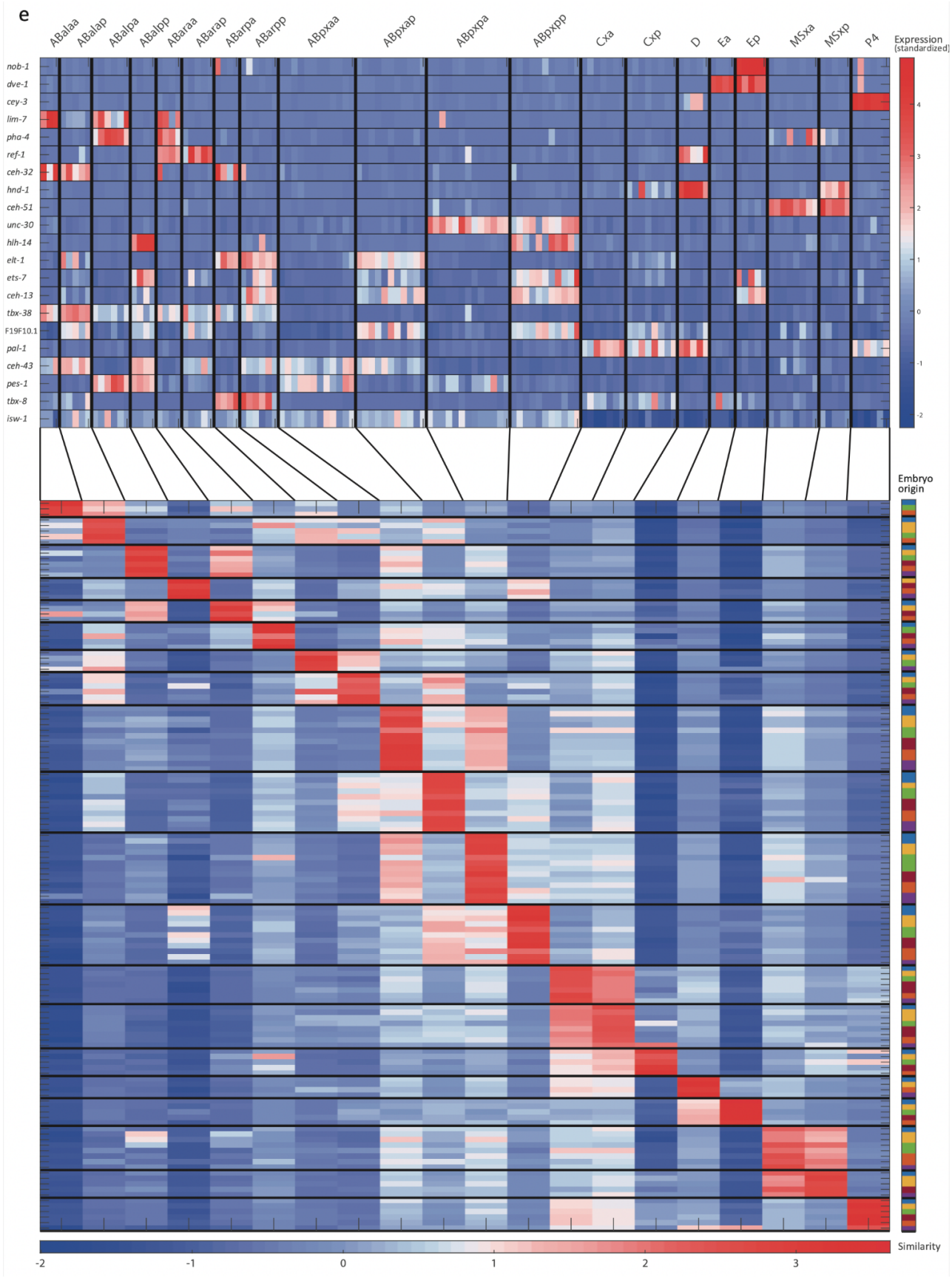
e
ABalaa
ABalap
ABalpa
ABalpp
ABaraa
ABarap
ABarpa
ABarpp
ABpxaa
ABpxap
ABpxpa
ABpxpp
Cxa
Cxp
D
Ea
Ep
MSxa
MSxp
P4
Expression (standardized)
nob-1
dve-1
cey-3
lim-7
pha-4
ref-1
ceh-32
hnd-1
ceh-51
unc-30
hlh-14
elt-1
ets-7
ceh-13
tbx-38
F19F10.1
pal-1
ceh-43
pes-1
tbx-8
isw-1
Embryo origin
Similarity
-2
-1
0
1
2
3

f

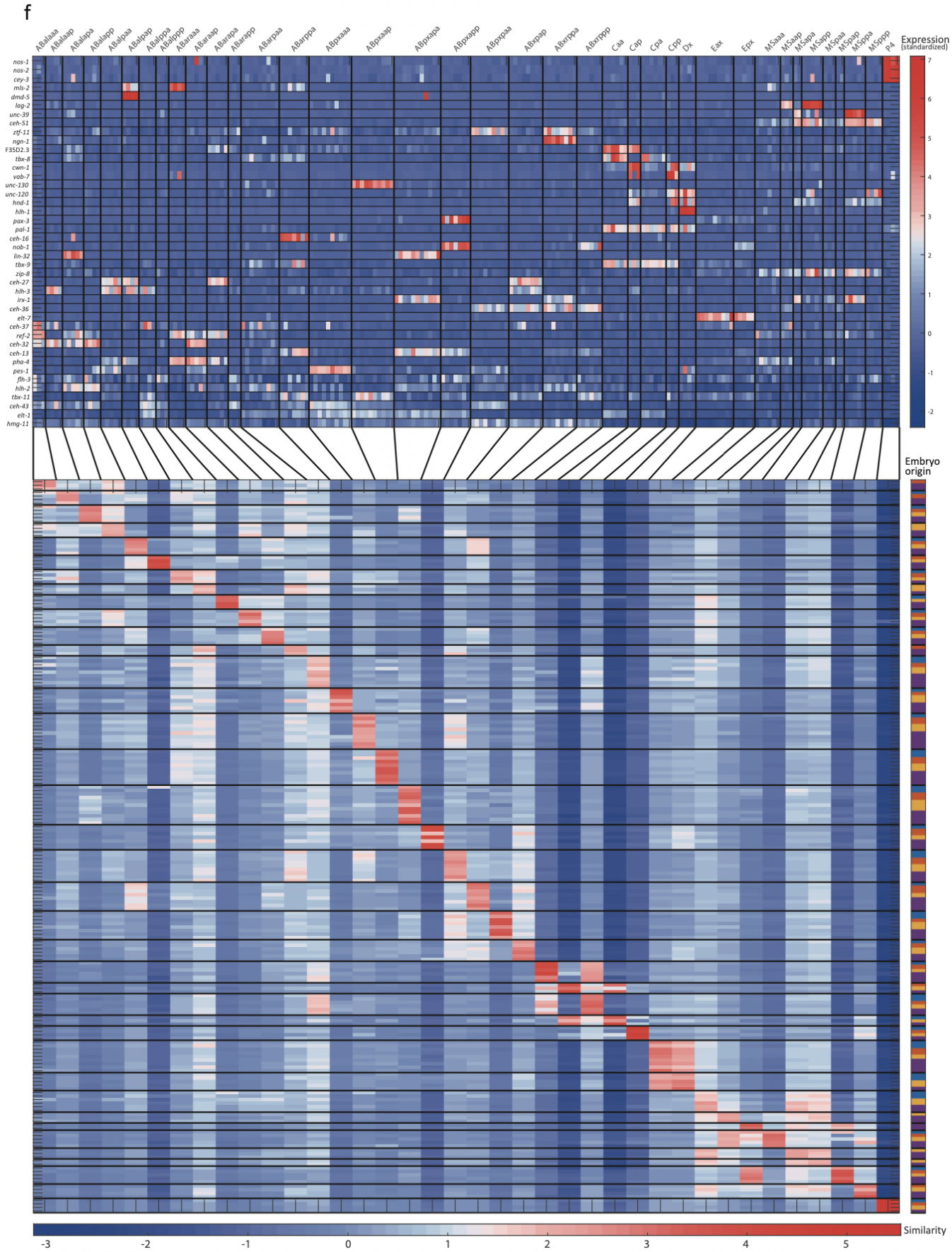
ABalaaa
ABalaap
ABalapa
ABalapp
ABalpaa
ABalpap
ABalppa
ABalppp
ABaraaa
ABaraap
ABarapa
ABarapp
ABarpaa
ABarppa
ABpxaaa
ABpxaap
ABpxapa
ABpxapp
ABpxpaa
ABpxpap
ABxrppa
ABxrppp
Caa
Cap
Cpa
Cpp
Dx
Eax
Epx
MSaaa
MSaap
MSapa
MSapp
MSpaa
MSpap
MSppa
MSppp
P4
nos-1
nos-2
cey-3
mls-2
dmd-5
lag-2
unc-39
ceh-51
ztf-11
ngn-1
F35D2.3
tbx-8
cwn-1
vab-7
unc-130
unc-120
hnd-1
hlh-1
pax-3
pal-1
ceh-16
nob-1
lin-32
tbx-9
zip-8
ceh-27
hlh-3
irx-1
ceh-36
elt-7
ceh-37
ref-2
ceh-32
ceh-13
pha-4
pes-1
flh-3
hlh-2
tbx-11
ceh-43
elt-1
hmg-11
Expression
(standardized)
7
6
5
4
3
2
1
0
-1
-2
Embryo
origin
Similarity
-3
-2
-1
0
1
2
3
4
5

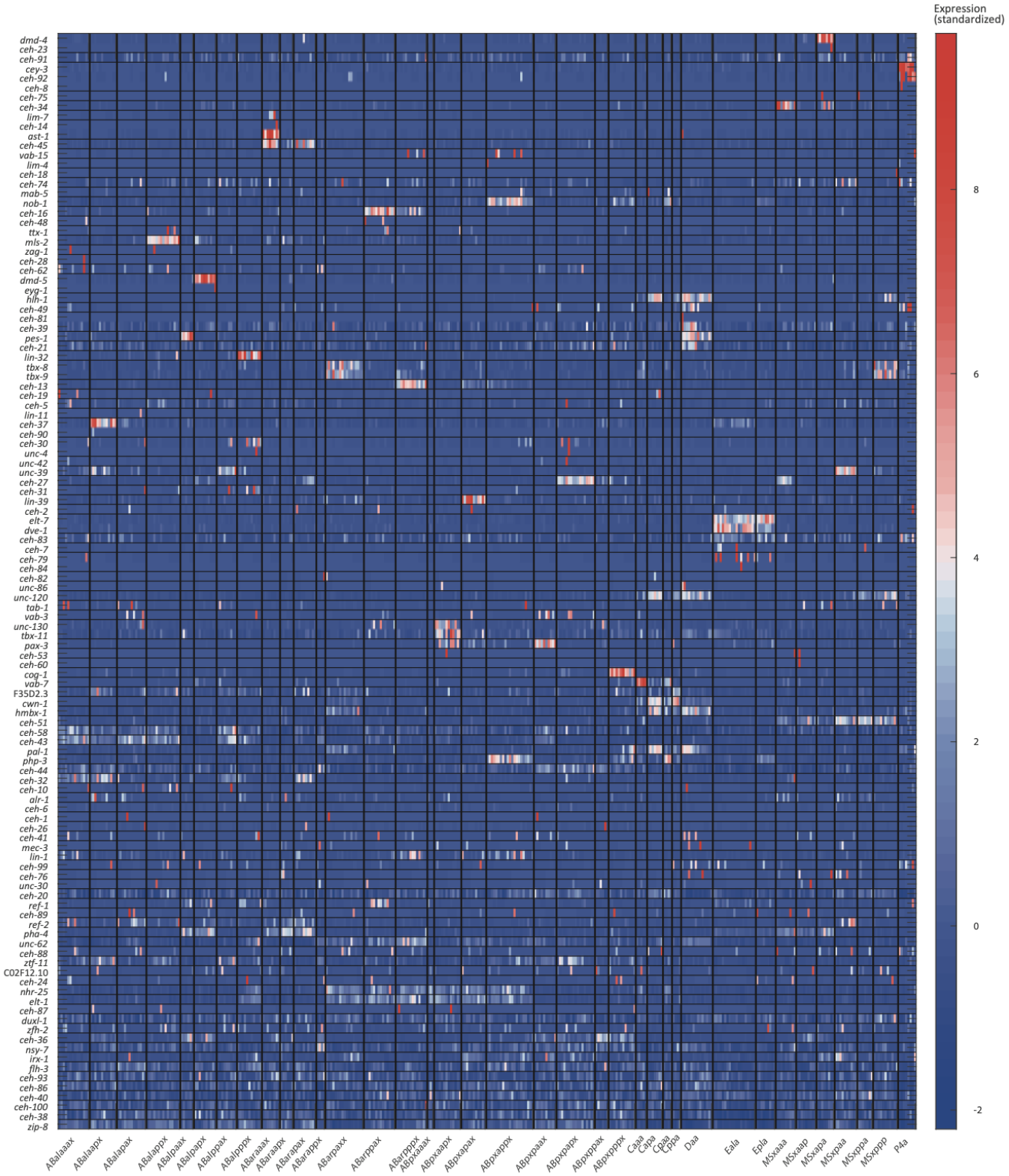
Expression (standardized)
8
6
4
2
0
-2
dmd-4
ceh-23
ceh-91
cey-3
ceh-92
ceh-8
ceh-75
ceh-34
lim-7
ceh-14
ast-1
ceh-45
vab-15
lim-4
ceh-18
ceh-74
mab-5
nob-1
ceh-16
ceh-48
ttx-1
mls-2
zag-1
ceh-28
ceh-62
dmd-5
eyg-1
hlh-1
ceh-49
ceh-81
ceh-39
pes-1
ceh-21
lin-32
tbx-8
tbx-9
ceh-13
ceh-19
ceh-5
lin-11
ceh-37
ceh-90
ceh-30
unc-4
unc-42
unc-39
ceh-27
ceh-31
lin-39
ceh-2
elt-7
dve-1
ceh-83
ceh-7
ceh-79
ceh-84
ceh-82
unc-86
unc-120
tab-1
vab-3
unc-130
tbx-11
pax-3
ceh-53
ceh-60
cog-1
vab-7
F35D2.3
cwn-1
hmbx-1
ceh-51
ceh-58
ceh-43
pal-1
php-3
ceh-44
ceh-32
ceh-10
alr-1
ceh-6
ceh-1
ceh-26
ceh-41
mec-3
lin-1
ceh-99
ceh-76
unc-30
ceh-20
ref-1
ceh-89
ref-2
pha-4
unc-62
ceh-88
ztf-11
C02F12.10
ceh-24
nhr-25
elt-1
ceh-87
duxl-1
zfh-2
ceh-36
nsy-7
irx-1
flh-3
ceh-93
ceh-86
ceh-40
ceh-100
ceh-38
zip-8
ABalaaax
ABalaapx
ABalapax
ABalappx
ABalpaax
ABalpapx
ABalppax
ABalpppx
ABaraaax
ABaraapx
ABarapax
ABarappx
ABarpaax
ABarppax
ABarpppx
ABpxaaax
ABpxaapx
ABpxapax
ABpxappx
ABpxpaax
ABpxpapx
ABpxppax
ABpxpppx
Caaa
Capa
Cpaa
Cppa
Daa
Eala
Epla
MSxaaa
MSxaap
MSxapa
MSxpaa
MSxppa
MSxppp
Paa

g2)

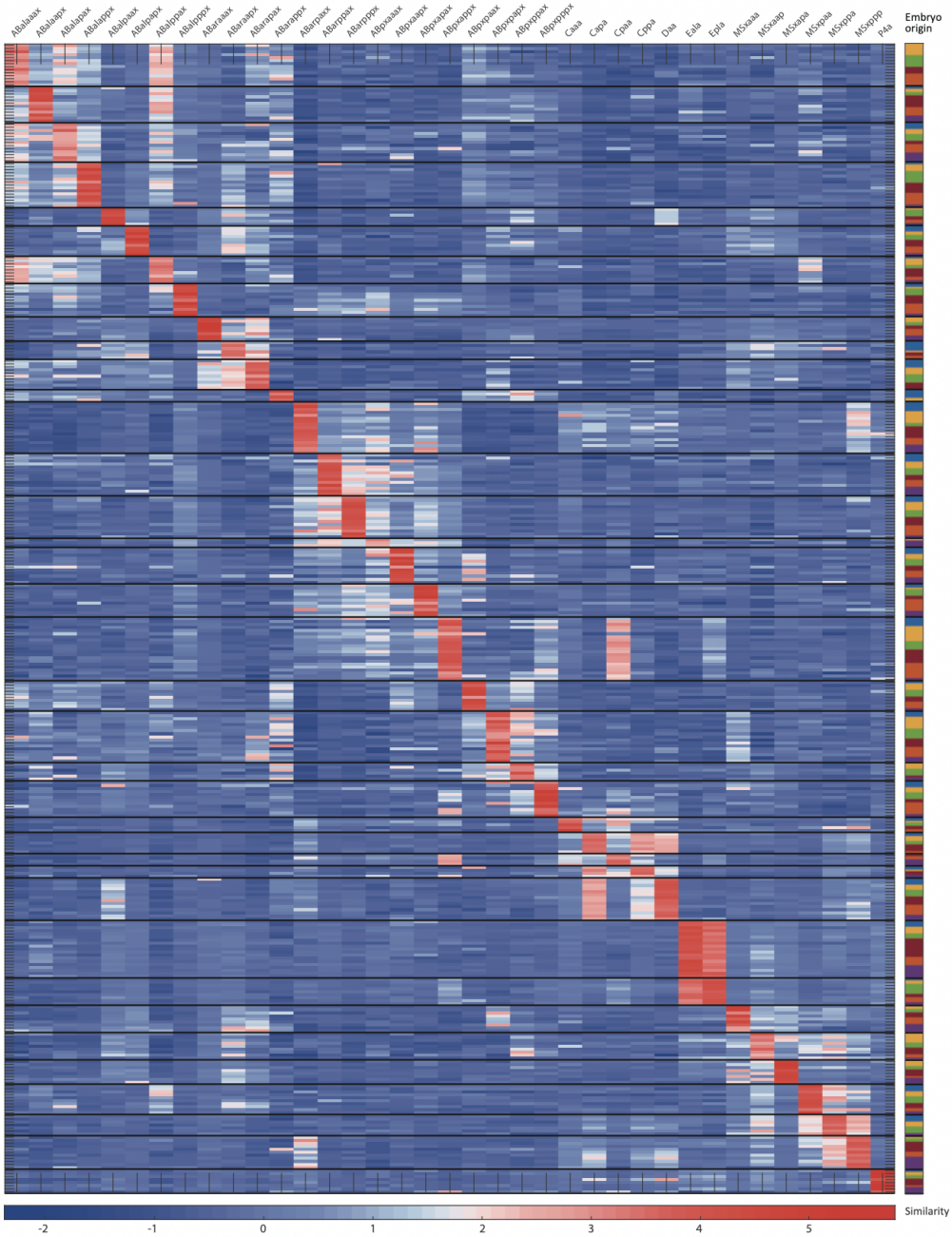

Figure S2: Cell state assignment and robustness analysis. For the 2-cell (**a**), 4-cell (**b**), 8-cell (**c**), 15-cell (**d**), 28-cell (**e**), 51-cell (**f**), and 102-cell (**g**) stages, the two plots indicate 1. the expression of known cell state markers (Tables S2 and S3) and 2. the similarity (correlation coefficient) across the cells in terms of these genes. Cells are colored by embryo of origin. Expression levels are indicated as z-scores. Cell states with a name including an 'x', indicate the multiple cell states with consistent name (Sulston et al., 1983). Cell similarity scores are shown by the colormap. To the right, the embryo of origin is indicated.

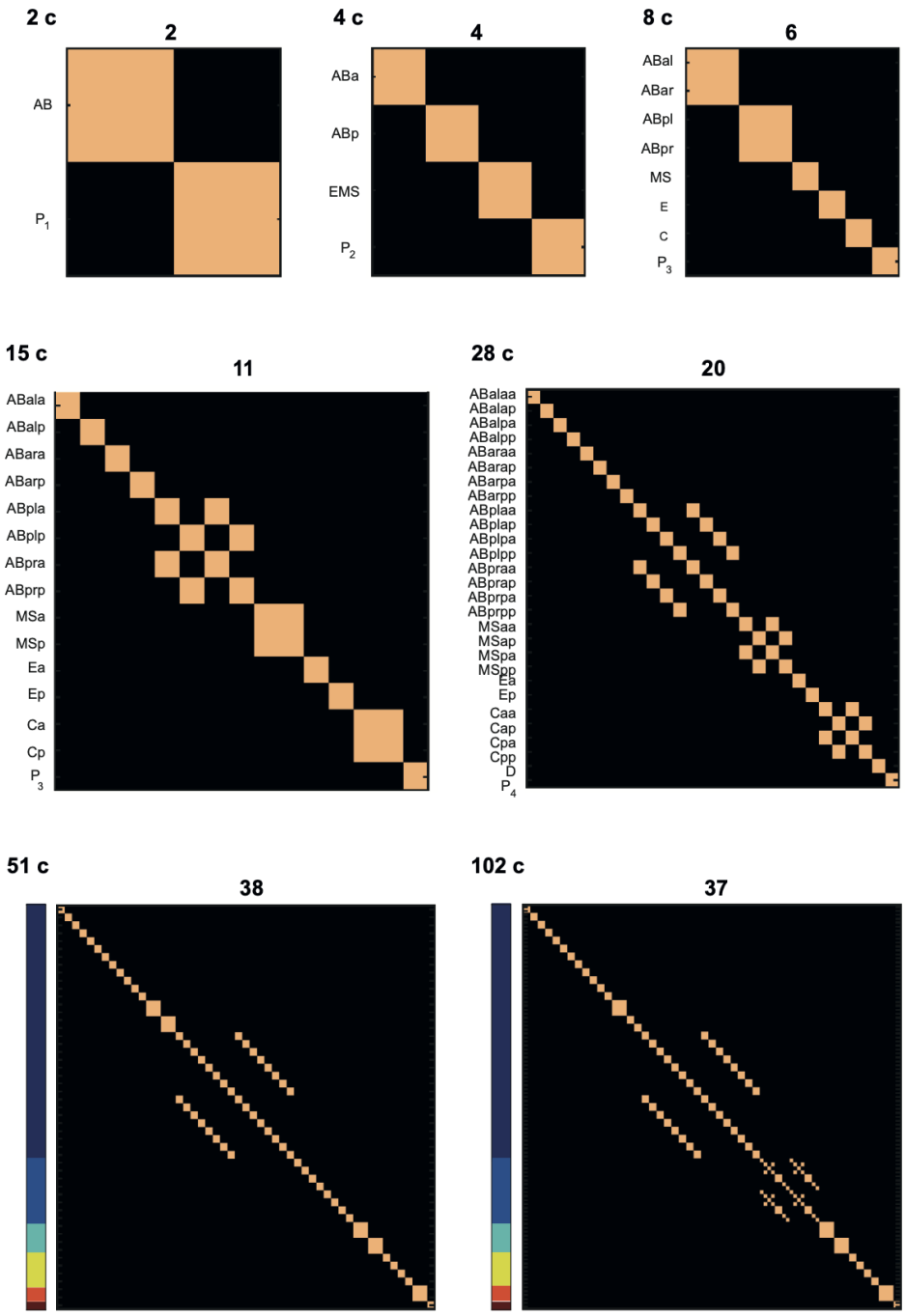

Figure S3: Number of cell states detected at each of the studied stages. Columns and rows correspond to cell identities (both in the same order). Light and dark colors correspond to identity and distinctness. For the 51 and 102 cell stages the cells are ordered same as in Figure 1 and 2. The number above each plot indicates the number of cell-states identified at the particular stage.

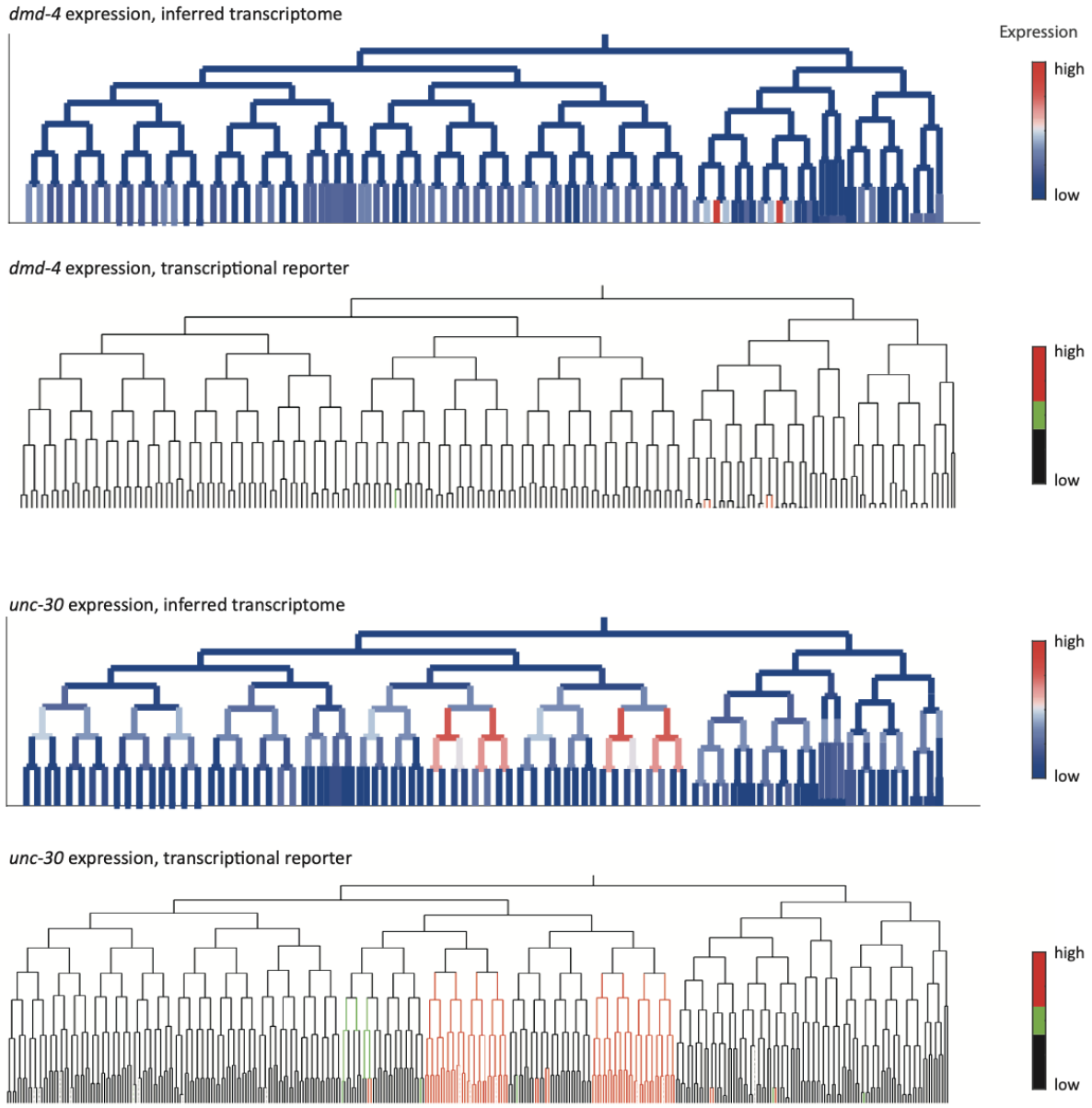

Figure S4: Inferred and validated gene expression. As in Fig. 2d, expression of *dmd-4* and *unc-30* according to lineage of the inferred transcriptomes (top) and a transcriptional reporter strain (bottom), where highest expression is shown in red and no detected expression is black.

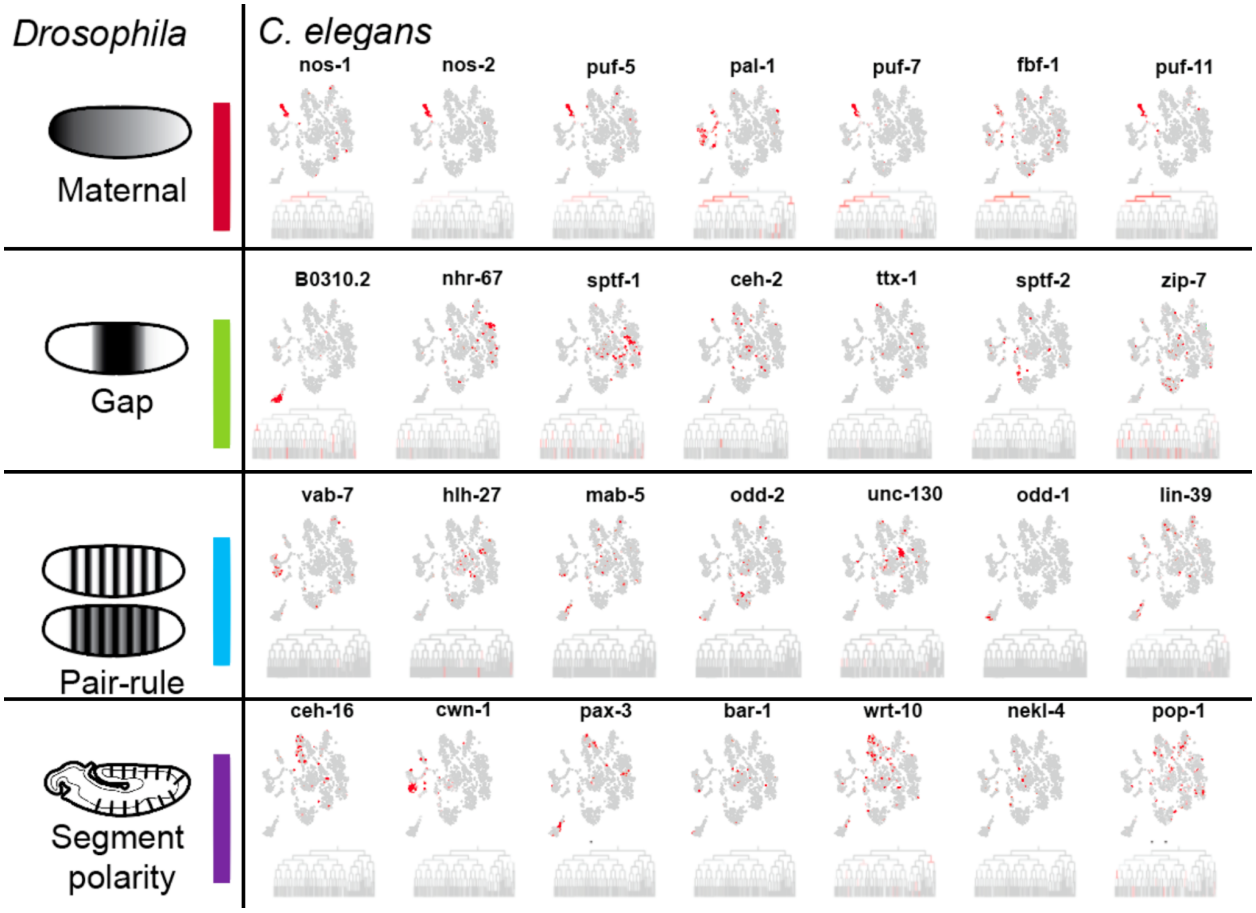

Figure S5: Expression of genes in C. elegans whose Drosophila orthologs have patterning functions. Expression on the tSNE plot is indicated as in Figure 1b.

SUPPLEMENTARY TABLES

Table S1: Characteristics of the dataset. Rows correspond to a studied embryo. The average number of transcripts and genes detected are shown.

Embryo ID	# Cells Collected	Intended Stage	# Transcripts	# Genes
1.1	1	1	501109	7110
1.2	1	1	145605	6138
1.3	1	1	245833	6605
2.1	2	2	90003	6337
2.3	2	2	79524	6249
2.4	2	2	69301	6110
2.5	2	2	76010	6186
4.1	4	4	57704	6827
4.3	4	4	52980	6603
4.5	4	4	502699	7776
7.1	7	8	256118	9980
8.1	7	8	270101	10102
8.2	6	8	251105	9525
8.3	7	8	243433	9938
8.4	8	8	275563	9819
10.1	10	8	244450	10501
13	11	15	121911	10600
13.2	11	15	146248	10173
14.2	14	15	183105	11323
15	11	15	143850	10532
17.2	17	15	138718	11363
22	21	28	149171	12485
23	20	28	129557	12078
24.1	24	28	139130	11762
24.2	23	28	91587	11562
25	23	28	82082	11406
27	26	28	113177	12007

45	41	51	60949	11840
48	48	51	51712	12066
48.2	42	51	35261	10977
51	38	51	42480	11675
55	53	51	48942	12409
72	68	102	44563	12249
82	76	102	38586	11743
88	83	102	38371	11874
92	90	102	39739	11900
96	96	102	44019	11855
96.2	75	102	26029	11555

Table S2: Gene markers from the literature. Cell state markers for the expression profiles used for assignment were curated from the literature (da Veiga Beltrame et al., 2022) and, in particular, one large study (Murray et al., 2012).

Gene	PMID	Title	Reference
mex-3	8861905	MEX-3 is a KH domain protein that regulates blastomere identity in early C. elegans embryos.	Cell. 1996 Oct 18;87(2):205-16.
oma-1	16611242	OMA-1 is a P granules-associated protein that is required for germline specification in Caenorhabditis elegans embryos.	Genes Cells. 2006 Apr;11(4):383-96
pes-10	7607073	Soma-germline asymmetry in the distributions of embryonic RNAs in Caenorhabditis elegans.	Development. 1994 Oct;120(10):2823-34.
cey-3	25487147	Spatiotemporal transcriptomics reveals the evolutionary history of the endoderm germ layer.	Nature. 2015 Mar 12;519(7542):219-22
end-3	12142026	Dynamics of a developmental switch: recursive intracellular and intranuclear redistribution of Caenorhabditis elegans POP-1 parallels Wnt-inhibited transcriptional repression.	Dev Biol. 2002 Aug 1;248(1):128-42.
hlh-26	15935776	The REF-1 family of bHLH transcription factors pattern C. elegans embryos through Notch-dependent and Notch-independent pathways.	Dev Cell. 2005 Jun;8(6):867-79.

mom-2	9288749	Wnt signaling polarizes an early C. elegans blastomere to distinguish endoderm from mesoderm.	Cell. 1997 Aug 22;90(4):695-705.
tbx-35	16831832	Specification of the C. elegans MS blastomere by the T-box factor TBX-35	Development. 2006 Aug;133(16):3097-106.
tbx-37	15056620	The T-box transcription factors TBX-37 and TBX-38 link GLP-1/Notch signaling to mesoderm induction in C. elegans embryos.	Development. 2004 May;131(9):1967-78.
tbx-38	15056620	The T-box transcription factors TBX-37 and TBX-38 link GLP-1/Notch signaling to mesoderm induction in C. elegans embryos.	Development. 2004 May;131(9):1967-78.
ceh-13	9334268	The expression of the C. elegans labial-like Hox gene ceh-13 during early embryogenesis relies on cell fate and on anteroposterior cell polarity.	Development. 1997 Nov;124(21):4193-200.
ceh-51	19605496	The NK-2 class homeodomain factor CEH-51 and the T-box factor TBX-35 have overlapping function in C. elegans mesoderm development.	Development. 2009 Aug;136(16):2735-46.
cey-3	25487147	Spatiotemporal transcriptomics reveals the evolutionary history of the endoderm germ layer.	Nature. 2015 Mar 12;519(7542):219-22

end-1	12142026	Dynamics of a developmental switch: recursive intracellular and intranuclear redistribution of Caenorhabditis elegans POP-1 parallels Wnt-inhibited transcriptional repression.	Dev Biol. 2002 Aug 1;248(1):128-42.
end-3	12142026	Dynamics of a developmental switch: recursive intracellular and intranuclear redistribution of Caenorhabditis elegans POP-1 parallels Wnt-inhibited transcriptional repression.	Dev Biol. 2002 Aug 1;248(1):128-42.
F19F10.1	Data	Figure 2	This work
hlh-26	15935776	The REF-1 family of bHLH transcription factors pattern C. elegans embryos through Notch-dependent and Notch-independent pathways.	Dev Cell. 2005 Jun;8(6):867-79.
pal-1	11133155	Zygotic expression of the caudal homolog pal-1 is required for posterior patterning in Caenorhabditis elegans embryogenesis.	Dev Biol. 2001 Jan 1;229(1):71-88.
ref-1	15935776	The REF-1 family of bHLH transcription factors pattern C. elegans embryos through Notch-dependent and Notch-independent pathways.	Dev Cell. 2005 Jun;8(6):867-79.
tbx-38	15056620	The T-box transcription factors TBX-37 and TBX-38 link GLP-1/Notch signaling to	Development. 2004 May;131(9):1967-78.

		mesoderm induction in C. elegans embryos.	
ceh-13	9334268	The expression of the C. elegans labial-like Hox gene ceh-13 during early embryogenesis relies on cell fate and on anteroposterior cell polarity.	Development. 1997 Nov;124(21):4193-200.
ceh-32	22508763	Multidimensional regulation of gene expression in the C. elegans embryo	http://epic.gs.washington.edu/Epic2/
ceh-43	22508763	Multidimensional regulation of gene expression in the C. elegans embryo	http://epic.gs.washington.edu/Epic2/
ceh-51	19605496	The NK-2 class homeodomain factor CEH-51 and the T-box factor TBX-35 have overlapping function in C. elegans mesoderm development.	Development. 2009 Aug;136(16):2735-46.
cey-3	25487147	Spatiotemporal transcriptomics reveals the evolutionary history of the endoderm germ layer.	Nature. 2015 Mar 12;519(7542):219-22
dve-1	22508763	Multidimensional regulation of gene expression in the C. elegans embryo.	Genome Res. 2012 Jul;22(7):1282-94.
elt-1	22508763	Multidimensional regulation of gene expression in the C. elegans embryo	http://epic.gs.washington.edu/Epic2/
ets-7	22508763	Multidimensional regulation of gene expression in the C. elegans embryo	http://epic.gs.washington.edu/Epic2/

hlh-14	22508763	Multidimensional regulation of gene expression in the C. elegans embryo	
hnd-1	22508763	Multidimensional regulation of gene expression in the C. elegans embryo	http://epic.gs.washington.edu/Epic2/
lim-7	22508763	Multidimensional regulation of gene expression in the C. elegans embryo	
ngn-1	22508763	Multidimensional regulation of gene expression in the C. elegans embryo	http://epic.gs.washington.edu/Epic2/
nob-1	22508763	Multidimensional regulation of gene expression in the C. elegans embryo.	Genome Res. 2012 Jul;22(7):1282-94.
pal-1	11133155	Zygotic expression of the caudal homolog pal-1 is required for posterior patterning in Caenorhabditis elegans embryogenesis.	Dev Biol. 2001 Jan 1;229(1):71-88.
pes-1	22508763	Multidimensional regulation of gene expression in the C. elegans embryo	http://epic.gs.washington.edu/Epic2/
pha-4	9649499	pha-4, an HNF-3 homolog, specifies pharyngeal organ identity in Caenorhabditis elegans.	Genes Dev. 1998 Jul 1;12(13):1947-52.
ref-1	22508763	Multidimensional regulation of gene expression in the C. elegans embryo	http://epic.gs.washington.edu/Epic2/
tbx-38	15056620	The T-box transcription factors TBX-37 and TBX-38 link GLP-1/Notch signaling to	Development. 2004 May;131(9):1967-78.

		mesoderm induction in C. elegans embryos.	
tbx-8	22508763	Multidimensional regulation of gene expression in the C. elegans embryo	http://epic.gs.washington.edu/Epic2/
unc-30	25738873	The Bicoid Class Homeodomain Factors ceh-36/OTX and unc-30/PITX Cooperate in C. elegans Embryonic Progenitor Cells to Regulate Robust Development.	PLoS Genet 11(3): e1005003
ceh-13	9334268	The expression of the C. elegans labial-like Hox gene ceh-13 during early embryogenesis relies on cell fate and on anteroposterior cell polarity.	Development. 1997 Nov;124(21):4193-200.
ceh-16	15659483	Ceh-16/engrailed patterns the embryonic epidermis of Caenorhabditis elegans	Development 132(4):739-49
ceh-27	22508763	Multidimensional regulation of gene expression in the C. elegans embryo	http://epic.gs.washington.edu/Epic2/
ceh-32	22508763	Multidimensional regulation of gene expression in the C. elegans embryo	http://epic.gs.washington.edu/Epic2/
ceh-36	25738873	The Bicoid Class Homeodomain Factors ceh-36/OTX and unc-30/PITX Cooperate in C. elegans Embryonic Progenitor Cells to	PLoS Genet 11(3): e1005003

		Regulate Robust Development.	
ceh-43	22508763	Multidimensional regulation of gene expression in the C. elegans embryo	http://epic.gs.washington.edu/Epic2/
ceh-51	19605496	The NK-2 class homeodomain factor CEH-51 and the T-box factor TBX-35 have overlapping function in C. elegans mesoderm development.	Development. 2009 Aug;136(16):2735-46.
elt-1	22508763	Multidimensional regulation of gene expression in the C. elegans embryo	http://epic.gs.washington.edu/Epic2/
elt-7	22508763	Multidimensional regulation of gene expression in the C. elegans embryo	http://epic.gs.washington.edu/Epic2/
hlh-1	22508763	Multidimensional regulation of gene expression in the C. elegans embryo	http://epic.gs.washington.edu/Epic2/
hlh-2	22508763	Multidimensional regulation of gene expression in the C. elegans embryo	http://epic.gs.washington.edu/Epic2/
hlh-3	22508763	Multidimensional regulation of gene expression in the C. elegans embryo	http://epic.gs.washington.edu/Epic2/
irx-1	22508763	Multidimensional regulation of gene expression in the C. elegans embryo	http://epic.gs.washington.edu/Epic2/
lag-2	22508763	Multidimensional regulation of gene expression in the C. elegans embryo	http://epic.gs.washington.edu/Epic2/

lin-32	22508763	Multidimensional regulation of gene expression in the C. elegans embryo	http://epic.gs.washington.edu/Epic2/
nob-1	22508763	Multidimensional regulation of gene expression in the C. elegans embryo	http://epic.gs.washington.edu/Epic2/
nos-2	10518502	nos-1 and nos-2, two genes related to Drosophila nanos, regulate primordial germ cell development and survival in Caenorhabditis elegans	DevelopmentVolume 126, Issue 21, November 1999, Pages 4861-4871
pal-1	11133155	Zygotic expression of the caudal homolog pal-1 is required for posterior patterning in Caenorhabditis elegans embryogenesis.	Dev Biol. 2001 Jan 1;229(1):71-88.
pax-3	22508763	Multidimensional regulation of gene expression in the C. elegans embryo	http://epic.gs.washington.edu/Epic2/
pes-1	22508763	Multidimensional regulation of gene expression in the C. elegans embryo	http://epic.gs.washington.edu/Epic2/
pha-4	22508763	Multidimensional regulation of gene expression in the C. elegans embryo	http://epic.gs.washington.edu/Epic2/
ref-1	15935776	The REF-1 family of bHLH transcription factors pattern C. elegans embryos through Notch-dependent and Notch-independent pathways.	Dev Cell. 2005 Jun;8(6):867-79.
ref-2	22508763	Multidimensional regulation of gene expression in the C. elegans embryo	http://epic.gs.washington.edu/Epic2/

tbx-11	22508763	Multidimensional regulation of gene expression in the C. elegans embryo	http://epic.gs.washington.edu/Epic2/
tbx-8	22508763	Multidimensional regulation of gene expression in the C. elegans embryo	http://epic.gs.washington.edu/Epic2/
tbx-9	22508763	Multidimensional regulation of gene expression in the C. elegans embryo	http://epic.gs.washington.edu/Epic2/
unc-120	22508763	Multidimensional regulation of gene expression in the C. elegans embryo	http://epic.gs.washington.edu/Epic2/
unc-130	22508763	Multidimensional regulation of gene expression in the C. elegans embryo	http://epic.gs.washington.edu/Epic2/
vab-7	22508763	Multidimensional regulation of gene expression in the C. elegans embryo	http://epic.gs.washington.edu/Epic2/
ztf-11	22508763	Multidimensional regulation of gene expression in the C. elegans embryo	http://epic.gs.washington.edu/Epic2/

Table S3: Expression of marker genes across cell identities [separate file]. For each cell state the expression of the cell state markers used for annotation (Table S2) is indicated.

Table S4: Inferred cell states. Each row corresponds to one of the 119 inferred cell states. The third column indicates the number of samples (scRNA-Seq cells) annotated to each cell state.

Cell-state	Cell identities	# cells
1	P_0	3
2	AB	4
3	P1	4
4	ABa	3

5	ABp	3
6	EMS	3
7	P2	3
8	ABal ABar	12
9	ABpl ABpr	11
10	MS	5
11	E	6
12	C	4
13	P3 (8-cell stage)	5
14	ABala	4
15	ABalp	5
16	ABara	4
17	ABarp	4
18	ABpla ABpra	9
19	ABplp ABprp	10
20	MSa MSp	12
21	Ea_15	3
22	Ep_15	4
23	Ca Cp	6
24	P3 (15-cell stage)	4
25	ABalaa	3
26	ABalap	5
27	ABalpa	6
28	ABalpp	4
29	ABaraa	4
30	ABarap	5
31	ABarpa	4
32	ABarpp	6
33	ABplaa ABpraa	12
34	ABplap ABprap	11
35	ABplpa ABprpa	13
36	ABplpp ABprpp	11

37	MSaa MSpa	8
38	MSap MSpp	5
39	Ea (28-cell stage)	4
40	Ep (28-cell stage)	5
41	Caa Cpa	7
42	Cap Cpp	8
43	D	5
44	P4 (28-cell stage)	6
45	ABalaaa	3
46	ABalaap	4
47	ABalapa	5
48	ABalapp	4
49	ABalpaa	5
50	ABalpap	4
51	ABalppa	4
52	ABalppp	3
53	ABaraaa	4
54	ABaraap	5
55	ABarapa	5
56	ABarapp	3
57	ABarpaa ABarpap	9
58	ABarppa ABarppp	7
59	ABplaaa ABpraaa	10
60	ABplaap ABpraap	10
61	ABplapa ABprapa	11
62	ABplapp ABprapp	7
63	ABplpaa ABprpaa	9
64	ABplpap ABprpap	8
65	ABplppa ABprppa	8
66	ABplppp ABprppp	6
67	MSaaa	6
68	MSaap	3

69	MSapa	2
70	MSapp	5
71	MSpaa	3
72	MSpap	2
73	MSppa	5
74	MSppp	4
75	Eal Ear	9
76	Epl Epr	5
77	Caa (51-cell stage)	6
78	Cap (51-cell stage)	3
79	Cpa (51-cell stage)	6
80	Cpp (51-cell stage)	3
81	Da Dp	4
82	P4 (51-cell stage)	4
83	ABalaaaa ABalaaap	14
84	ABalaapa ABalaapp	12
85	ABalapaa ABalapap	13
86	ABalappa ABalappp	15
87	ABalpaaa ABalpaap	6
88	ABalpapa ABalpapp	10
89	ABalppaa ABalppap	9
90	ABalpppa ABalpppp	11
91	ABaraaaa ABaraaap	8
92	ABaraapa ABaraapp	6
93	ABarapaa ABarapap	10
94	ABarappa ABarappp	4
95	ABarpaaa ABarpaap ABarpapa ABarpapp	17
96	ABarppaa ABarppap	14
97	ABarpppa ABarpppp	14
98	ABplaaaa ABplaaap ABpraaaa ABpraaap	3
99	ABplaapa ABplaapp ABpraapa ABpraapp	12

100	ABplapaa ABplapap ABprapaa ABprapap	11
101	ABplappa ABplappp ABprappa ABprappp	21
102	ABplpaaa ABplpaap ABprpaaa ABprpaap	10
103	ABplpapa ABplpapp ABprpapa ABprpapp	17
104	ABplppaa ABplppap ABprppaa ABprppap	6
105	ABplpppa ABplpppp ABprpppa ABprpppp	12
106	MSaaaa MSpaaa	9
107	MSaaap MSaapp MSpaap MSpapp	9
108	MSaapa MSpapa	8
109	MSapaa MSapap MSppaa MSppap	10
110	MSappa MSpppa	7
111	MSappp MSpppp	11
112	Eala Ealp Eara Earp	19
113	Epla Eplp Epra Eprp	9
114	Caaa Caap	5
115	Capa Capp	7
116	Cpaa Cpap	4
117	Cppa Cppp	4
118	Daa Dap Dpa Dpp	14
119	P4a P4p (102-cell stage)	8

Table S5: Cell state assignments [separate file]. For each sample (scRNA-Seq), the table provides the GEO accession number, sample name, embryo ID, annotated cell state, and the number of transcripts detected.

Table S6: Gene expression dataset [separate file]. For each gene, the average, standardized, differential, and standard deviation of expression is provided (see Methods) across the 119 detected cell states.